

**This is the accepted manuscript version of the contribution  
published as:**

Cárdenas, P., Lange, C.B., Vernet, M., Esper, O., Srain, B., Vorrath, M.-E., **Ehrhardt, S.**, Müller, J., Kuhn, G., Arz, H.W., Lembke-Jene, L., Lamy, F. (2019):  
Biogeochemical proxies and diatoms in surface sediments across the Drake Passage reflect oceanic domains and frontal systems in the region  
*Prog. Oceanogr.* **174** , 72 – 88

**The publisher's version is available at:**

<http://dx.doi.org/10.1016/j.pocean.2018.10.004>

## Accepted Manuscript

Biogeochemical proxies and diatoms in surface sediments across the Drake Passage reflect oceanic domains and frontal systems in the region

Paola Cárdenas, Carina B. Lange, Maria Vernet, Oliver Esper, Benjamin Srain, Maria-Elena Vorrath, Sophie Ehrhardt, Juliane Müller, Gerhard Kuhn, Helge W. Arz, Lester Lembke-Jene, Frank Lamy

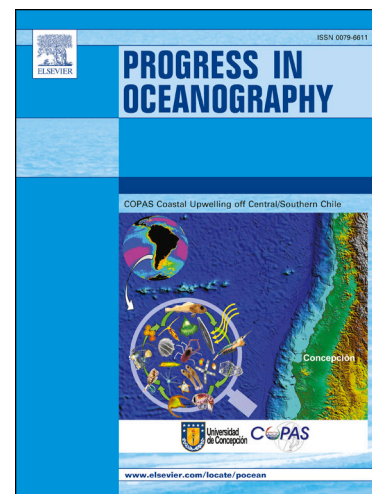
PII: S0079-6611(18)30190-3  
DOI: <https://doi.org/10.1016/j.pocean.2018.10.004>  
Reference: PROOCE 2019

To appear in: *Progress in Oceanography*

Received Date: 22 June 2018  
Revised Date: 20 September 2018  
Accepted Date: 4 October 2018

Please cite this article as: Cárdenas, P., Lange, C.B., Vernet, M., Esper, O., Srain, B., Vorrath, M-E., Ehrhardt, S., Müller, J., Kuhn, G., Arz, H.W., Lembke-Jene, L., Lamy, F., Biogeochemical proxies and diatoms in surface sediments across the Drake Passage reflect oceanic domains and frontal systems in the region, *Progress in Oceanography* (2018), doi: <https://doi.org/10.1016/j.pocean.2018.10.004>

This is a PDF file of an unedited manuscript that has been accepted for publication. As a service to our customers we are providing this early version of the manuscript. The manuscript will undergo copyediting, typesetting, and review of the resulting proof before it is published in its final form. Please note that during the production process errors may be discovered which could affect the content, and all legal disclaimers that apply to the journal pertain.



**Biogeochemical proxies and diatoms in surface sediments across the Drake Passage reflect oceanic domains and frontal systems in the region**

Paola Cárdenas<sup>a, b, c</sup>, Carina B. Lange<sup>\*b, c, d</sup>, Maria Vernet<sup>e</sup>, Oliver Esper<sup>f</sup>, Benjamin Srain<sup>b</sup>, Maria-Elena Vorrath<sup>f</sup>, Sophie Ehrhardt<sup>g</sup>, Juliane Müller<sup>f, h</sup>, Gerhard Kuhn<sup>f</sup>, Helge W. Arz<sup>i</sup>, Lester Lembke-Jene<sup>f</sup>, Frank Lamy<sup>f</sup>

<sup>a</sup>Programa de Postgrado en Oceanografía, Departamento de Oceanografía, Facultad de Ciencias Naturales y Oceanográficas, Universidad de Concepción, Concepción, Chile

<sup>b</sup>Centro Oceanográfico COPAS Sur-Austral, Universidad de Concepción, Concepción, Chile

<sup>c</sup>Centro de Investigación Dinámica de Ecosistemas Marinos de Altas Latitudes (IDEAL), Universidad Austral de Chile, Valdivia, Chile

<sup>d</sup>Departamento de Oceanografía, Universidad de Concepción, Chile

<sup>e</sup>Scripps Institution of Oceanography, University of California San Diego, La Jolla, California 92093-0218, USA

<sup>f</sup>Alfred-Wegener Institut, Helmholtz Zentrum für Polar and Meeresforschung, Bremerhaven, Germany

<sup>g</sup>Helmholtz-Zentrum für Umweltforschung – UFZ, Leipzig, Germany

<sup>h</sup>Universität Bremen, Zentrum für Marine Umweltwissenschaften MARUM, Bremen, Germany

<sup>i</sup>Leibniz-Institut für Ostseeforschung Warnemünde (IOW), Rostock-Warnemünde, Germany

\*Corresponding author: [clang@udec.cl](mailto:clang@udec.cl)

**Abstract**

The Antarctic Circumpolar Current is the world's largest current system connecting all major ocean basins of the global ocean. Its flow, driven by strong westerly winds, is constricted to its narrowest extent in the Drake Passage, located between South America and the Antarctic Peninsula. Due to the remoteness of the area, harsh weather conditions and strong bottom currents, sediment recovery is difficult and data coverage is still inadequate. Here, we report on the composition of 51 surface sediments collected during the R/V Polarstern PS97 expedition (February–April 2016) across the western and central Drake Passage, from the Chilean/Argentinian continental margin to the South Shetland Islands and the Bransfield Strait (water depth: ~100–4000 m). We studied microfossils (diatoms), bulk sediment composition and geochemical proxies (biogenic opal, organic carbon, calcium carbonate, carbon and nitrogen stable isotopes, sterols and photosynthetic pigments), and evaluated how they respond to, and reflect oceanic domains and polar to subpolar frontal systems in this region. Our multi-proxy approach shows a strong relationship between the composition of surface sediments and ocean productivity, terrigenous input, intensity of ocean currents, and ice proximity, clearly differentiating among 4 biogeographical zones. The Subantarctic Zone was characterized by warmer-water diatoms, high carbonate (>45%) and low organic carbon contents (avg. 0.26%), as well as low concentrations of pigments (avg. 1.75  $\mu\text{g/g}$ ) and sterols (avg. 0.90  $\mu\text{g/g}$ ). A general N-S transition from carbonate-rich to opal-rich sediment was observed at Drake Passage sites of the Polar Front and Permanently Open Ocean Zone. These sites were characterized by low organic carbon content (0.22%), high relative abundances of heavily silicified diatoms ( $\geq 60\%$  *Fragilariopsis kerguelensis*), and abundant foraminifera at shallower stations. Approaching the Antarctic Peninsula in the Transitional Zone, an increase in the concentrations of pigments and sterols (avg. 2.57  $\mu\text{g/g}$  and 1.44  $\mu\text{g/g}$ , respectively) and a strong decrease in carbonate content was observed. The seasonal Sea-Ice Zone

in the southern section of the study area, had the highest contents of biogenic opal (avg. 14.6%) and organic carbon (avg. 0.7%), low carbonate contents (avg. 2.4%), with the occurrence of sea-ice-related diatoms and sterols. In all zones, terrigenous input was detected, although carbon/nitrogen ratios and  $\delta^{13}\text{C}_{\text{org}}$  suggest a predominance of marine-derived organic matter; lower values of  $\delta^{13}\text{C}_{\text{org}}$  occurred south of the Polar Front. The new results presented here constitute a highly valuable reference dataset for the calibration of microfossil and geochemical proxies against observational data and provide a useful regional baseline for future paleo-research.

Keywords: Drake Passage, surface sediments, organic carbon, photosynthetic pigments, sterols, diatoms

## 1. Introduction

The Southern Ocean (SO) plays an essential role in the Earth's climate and biogeochemical cycles, regulating both the circulation of nutrients in the ocean and CO<sub>2</sub> concentrations in the atmosphere (e.g., Marinov et al., 2006; Frölicher et al., 2015; Rintoul, 2018). The dominant feature of the SO is the eastward-flowing Antarctic Circumpolar Current (ACC). It is the world's largest current system, driven by strong westerly winds. It connects the Atlantic, Pacific, and Indian ocean basins, allowing for inter-basin exchange of heat, salt, carbon, and other chemical and biological properties while thermally isolating Antarctica by limiting poleward meridional heat transport (Toggweiler and Bjornsson, 2000; Meredith et al., 2011; Ladant et al., 2018; Rintoul, 2018).

Three primary oceanographic fronts in the SO separate major zones of relatively uniform water properties, and distinct phytoplankton chlorophyll levels and species assemblages. The Subantarctic Front (SAF) marks the southernmost limit of relatively warm subantarctic surface water; the Polar Front (PF) is the boundary between the relatively warmer subantarctic and the cold Antarctic waters, defined as the northernmost extent of the 2°C isotherm at 200 m depth; and the southern ACC Front (SACCF), which often coincides with the seasonal maximum sea-ice extent (e.g., Orsi et al., 1995; Sprintall, 2003; Kim and Orsi, 2014; Giglio and Johnson, 2016; Nghiem et al., 2016). The flow of the ACC and the position of the SAF and PF are strongly influenced by bottom topography, and in the DP, the fronts are closely spaced (Fig. 1). The fronts are characterized by large geostrophic surface velocities and are associated with deep-reaching jets and the subduction or upwelling of different water masses (e.g., Orsi et al., 1995; Carter et al., 2009; Sokolov and Rintoul, 2009).

The surface waters of the Subantarctic Zone (SAZ), located between the Subtropical Front and the SAF are defined as a carbonate-dominated regime with coccolithophores accompanied by cyanobacteria and dinoflagellates; diatom production and export flux are relatively low (e.g.,

Honjo, 2004; Rigual-Hernández et al., 2015). The Polar Front Zone (PFZ) lies between the SAF and the PF and is characterized by a subsurface chlorophyll maximum dominated by high abundances of large diatoms (Kopczynska et al., 2001). To the south, the Permanently Open Ocean Zone (POOZ) stretches from the PF to the northern limit of the winter sea ice extent. It is an area with strong seasonality in biological production (Moore and Abbott, 2000) where waters are predominantly high-nutrient low-chlorophyll (HNLC; e.g., Martin et al., 1990; Venables and Moore, 2010), except where iron is supplied to the surface ocean (i.e., downstream of islands and where fronts interact with large bathymetric features; Pollard et al., 2006; Ardelan et al., 2010; Frants et al., 2013; Wadley et al., 2014). The Antarctic Zone (AZ) lies south of the SACCF (e.g., Sokolov and Rintoul, 2007; Rintoul, 2009; Deppeler and Davidson, 2017). It can further be subdivided into the seasonal Sea-Ice Zone (sSIZ), where sea-ice supports a diverse community of algae; the Marginal Ice Zone, with high productivity in spring-summer; and the Antarctic Continental Shelf Zone, characterized by high productivity with blooms supporting abundant and diverse Antarctic life (see review in Deppeler and Davidson, 2017).

Wind-driven upwelling in the SO allows nutrient-rich Upper Circumpolar Deep Water to rise to the surface, providing dissolved inorganic nutrients to the upper water column (e.g., Pollard et al., 2006). These support biological production (Sarmiento et al., 2004), which leads to CO<sub>2</sub> uptake from the atmosphere (Anderson et al., 2002; Morrison et al., 2015). The upwelled deep waters are then transformed into intermediate (Antarctic Intermediate Water) and mode waters (Subantarctic Mode Water) and are subducted northward across the PF and SAF to lower latitudes (e.g., Sarmiento et al., 2004; Anderson et al., 2009, Marshall and Speer, 2012). The supply of dissolved nutrients to surface waters by upwelling is greatest just south of the PF; silicic acid is stripped out preferentially over nitrate as the water moves north (Sarmiento et al., 2004; Anderson et al., 2009; Chase et al., 2015); thus, Si concentrations differ markedly from north to

south (e.g., Subantarctic waters 1–5  $\mu\text{M}$  vs. as high as Si  $\sim 60 \mu\text{M}$  south of the PFZ; Coale, 2004).

The large amounts of silicic acid at the surface (Trull et al., 2001) are converted to biogenic Si, primarily by diatoms (e.g., Nelson et al., 2002; Tréguer and De La Rocha, 2013). Diatom export production in the SO is reflected in the underlying sediments in the form of a band of siliceous ooze, the opal belt that preserves one-third of the world's biogenic Si (Cortese et al., 2004; Geibert et al., 2005; Tréguer and De La Rocha, 2013; Tréguer, 2014). This belt is not continuous, and a break occurs in the Drake Passage (DP) (Chase et al., 2015; Dutkiewicz et al., 2015).

The DP, located between Cape Horn (the most southerly point of South America) and the Antarctic Peninsula, is the narrowest constriction ( $\sim 800$  km) through which the ACC must pass on its way to the east around the SO. Through the DP, cool, low-salinity waters return to the Atlantic, affecting the strength of the Atlantic meridional overturning circulation, together with saline subtropical Indian Ocean waters that enter at the Agulhas Retroflexion (cold- and warm-water routes, respectively; Gordon, 1986; Beal et al., 2011).

Most previous knowledge on the texture and composition of seafloor sediments and sediment cores taken across the entire DP area comes from the USNS Eltanin expeditions carried out in the 1960s (Goodell, 1964; 1965; see Herb, 1968, 1971 for foraminifera studies in surface sediments). Severe weather conditions and strong bottom currents make the recovery of sediment records within the DP difficult. Thus, marine sediment coverage and data are still sparse in this area; most are restricted to the southernmost South American continental margin (e.g., Caniupán et al., 2011; Harada et al., 2013; Lamy et al., 2015) and, in particular, to the Antarctic Peninsula area (e.g., Domack et al., 2001, 2003; Heroy et al., 2008; Milliken et al., 2009; Yoon et al., 2009; Hass et al., 2010; Majewski et al., 2012; Isla, 2016; Veit-Köhler et al., 2018).

The goal of this study was to determine if the biogeochemical composition of surface sediments across the DP – from the Chilean/Argentinian continental margin to the South Shetland

Islands (SSI) and the Bransfield Strait (BS) – reflects the oceanic domains, environmental gradients, and polar to subpolar frontal systems in this remote and understudied region. We base our evaluation on a multi-proxy approach including: biogenic opal, total organic carbon (TOC), and calcium carbonate ( $\text{CaCO}_3$ ), as proxies for biological export production; C/N ratios and stable carbon isotope signatures of organic carbon for tracing sources of organic matter; and diatom species assemblages and their geographical distribution as proxies for environmental gradients. We also deliver novel results on sedimentary photosynthetic pigments and sterols; the former is used as an estimator of euphotic zone biomass and early diagenetic processes, whereas the diversity of sterols helps in assigning their different biological sources. We show that the biogeochemical composition of the surface sediments varies latitudinally according to oceanographic conditions that are mostly determined by oceanographic fronts and sea-ice dynamics close to Antarctica. By enlarging the data coverage in this sparsely sampled region, we contribute towards establishing a useful regional baseline for future paleo-studies.

## 2. Study area

Our study covers an extensive geographical area (Fig. 1). Along the Chilean margin south of 45°S, the narrow (extending 100–150 km offshore) and strong (velocities of 15–35 cm/s) Cape Horn Current transports low salinity and modified ACC waters into the Atlantic through the northern DP (Chaigneau and Pizarro, 2005). This area is characterized by a strong latitudinal gradient in sea surface temperature and salinity, high concentrations of dissolved oxygen (Provost et al., 2011), and high inputs of dissolved iron from fluvial and glacial Patagonian sources (Klunder et al., 2014; Paparazzo et al., 2016).

Since the 1970s, numerous oceanographic surveys across the DP have contributed to our understanding of seasonal and interannual variability in ACC transport (see reviews by Meredith et al., 2011 and Sprintall et al., 2012). The majority of the ACC transport is associated with the SAF and PF, whose positions are determined by the location of maximum westerly wind stress and the rough bottom topography of the DP (i.e., Shackleton Fracture Zone; e.g., Meredith et al., 2011; Ferrari et al., 2014; Donohue et al., 2016). Local maxima in eddy kinetic energy are observed in the northern half of the DP; these eddies may constitute an efficient mechanism for meridional heat flux across the DP (Barré et al., 2011; Ferrari et al., 2014). Although biological parameters have not been measured with the same density and intensity as hydrological properties in the DP, changes over time and space have been observed (Munro et al., 2015 a,b; Eveleth et al., 2017). Phytoplankton blooms in the DP typically occur in austral spring (e.g., Demidov et al., 2011), although Gradone (2016) revealed the presence of both a spring and a fall bloom between 2012 and 2015, using underway fluorometer-derived chlorophyll data along with satellite-derived chl  $a$  estimates from the MODIS sensor. Zooplankton (from a 1999–2004 time-series acoustic backscatter) has a well-defined annual cycle, moving from a late-winter minimum to a spring-summer maximum (Chereskin and Tarling, 2007), and a higher density and biomass of copepods is seen in Subantarctic rather than in Antarctic waters (Thompson et al., 2012).

Hendry et al. (2018) have recently reviewed the marine ecosystem of the West Antarctic Peninsula (WAP). Close to the Peninsula, hydrographic surveys have contributed to the knowledge of water mass structure and circulation patterns in the region comprising the southern DP, SSI and the BS (see review by Moffat and Meredith, 2018). Surface waters in the BS have two main sources: from the southwest, the Bellingshausen Sea provides warm, relatively fresh waters which flow northeastward inside the BS along the southern slope of the SSI; and the Weddell Sea supplies a large amount of cold (below 0°C) and dense water (e.g., Gordon and Nowlin, 1978;

Sangrà et al., 2011, 2017). The slope of the SSI is occupied by fresher and warmer (above  $-0.4^{\circ}\text{C}$ ) waters spanning about two-thirds of the strait's width (Moffat and Meredith, 2018). Dissolved iron concentrations are high over the shelf off the Antarctic Peninsula and the SSI (Klunder et al., 2014; Meredith et al., 2018), making it a highly productive ecosystem. Primary production over the WAP shelf is related to sea-ice dynamics (Vernet et al., 2008), and phytoplankton blooms (i.e., diatoms, colonial haptophyte *Phaeocystis*) are common throughout spring and summer, consistently occurring in Marguerite Bay and the Bellingshausen Sea areas (Marrari et al., 2008). Near the shelf break and in coastal waters along the northern Antarctic Peninsula, phytoplankton bloom development seems to be controlled by the upwelling of iron-rich deep water (Marrari et al., 2008). The northern shelf of the SSI and the BS are important areas for both the krill fishery and krill-dependent predators (Hinke et al., 2017).

### 3. Material and Methods

#### 3.1 Sampling

We analyzed 51 surface sediment samples collected during the R/V Polarstern expedition PS97 "PaleoDrake" in 2016. The expedition's sampling scheme included the Chilean/Argentinian continental margin, two N-S transects across the western and central DP, and the SSI and the BS area (Fig. 1; Lamy, 2016).

In contrast to the sediments from earlier campaigns with R/V Eltanin across the DP, which were retrieved with an Ewing corer, as short phleger cores or grab samples (Goodell, 1964; 1965) and may have suffered from considerable loss at the core-top, our new dataset consists of surface samples carefully recovered with a Multicorer sampling device (MUC, 45 stations) and a giant box corer (GKG; 6 stations in the SSI area) (Table S1). Only cores with an intact surface and a water

layer on top of the sediment were sampled onboard, immediately after recovery, and stored at -80°C to avoid e.g., photo-oxidation and the degradation of pigments and biomarkers. All samples used in this study represent the upper 1-cm of surface sediment. Given the contrasting depositional environments of our study area, the surface sediments do not necessarily represent “modern” deposition and may integrate over different times.

Initial micropaleontological and sedimentological information was obtained at each station during the cruise (Lamy, 2016; Lange et al., 2016). Onboard sediment acoustic profiles taken with a PARASOUND sub-bottom profiling system documented the absence of, or very sparse sediment cover between the SAF and the PF (Lamy, 2016) in the Hero Fracture Zone (no samples; Fig. 1), whereas sediment cover slightly increased in the central DP just north of the PF, along the Shackleton Fracture Zone (station PS97/089). Both, the Hero and Shackleton Fracture zones rise several hundred to thousands of meters above the surrounding seafloor and form the main bathymetric characteristics of the DP.

The geographical distribution of the sampling stations falls within the following oceanographic zones, broadly following descriptions by Rigual-Hernández et al. (2015) and Deppeler and Davidson (2017): (a) The SAZ includes 17 sites on the Chilean/Argentinian continental margins and 3 offshore sites. (b) Due to the sparse coverage of surface samples between the SAF and the PF, we combine the PFZ with the POOZ sites (14) into one large, open-ocean zone termed PFZ+POOZ encompassing the western and central DP. (c) Approaching the Antarctic Peninsula, 3 sites from the continental margin represent a “transitional zone” (TZ) between the open DP and the SSI-BS area. d) Finally, we include the 14 sites in the SSI-BS region into the sSIZ.

### *3.2 Sediment composition*

Total carbon (TC) and nitrogen (TN) contents were analyzed using a CNS analyzer (Elementar Vario EL III) at the Alfred Wegener Institute (AWI) in Bremerhaven on freeze-dried and homogenized sediments. Total organic carbon (TOC) contents were determined with a carbon-sulfur determinator (CS-2000, ELTRA) after the removal of inorganic carbon (TIC, carbonates) by adding hydrochloric acid.

The percentage of carbonate was calculated from the difference between the amount of total carbon and organic carbon, using the following equation:  $\text{CaCO}_3 \text{ (wt.\%)} = (\text{TC} - \text{TOC}) \times 8.333$ .

The C/N ratio was calculated as:  $(\text{TOC wt.\%} / \text{C atomic mass}) / (\text{TN} / \text{N atomic mass})$ .

Biogenic opal was estimated following the alkaline extraction procedure described by Mortlock and Froelich (1989), but using NaOH as a digestion solution (Müller and Schneider, 1993). Fifty milligrams of freeze-dried sediment were first treated with 10 %  $\text{H}_2\text{O}_2$  and 1 N HCl, and then extracted with 1 M NaOH (40 ml; pH ~13) at 85°C for 5 hours. Extraction and analysis by molybdate-blue spectrophotometry were conducted at the Laboratories of Marine Organic Geochemistry and Paleoceanography, University of Concepción, Chile. Values are expressed as biogenic opal by multiplying the Si (%) by 2.4 (Mortlock and Froelich, 1989).

Percentages of siliciclastic material were estimated as:

$100 \text{ wt.\%} - (\text{CaCO}_3 \text{ wt.\%} + 2 \times \text{TOC wt.\%} + \text{biogenic opal wt.\%})$ .

All parameters were porewater salt corrected (Kuhn, 2013).

### 3.3 Stable isotopes

Carbon ( $\delta^{13}\text{C}_{\text{org}}$ ) and nitrogen ( $\delta^{15}\text{N}$ ) stable isotopes were measured on freeze-dried surface sediment samples (~100 mg) at the Bioanalytical Laboratory, School of Biological Sciences, Washington State University, USA. An elemental analyzer coupled with an Isoprime isotope ratio mass spectrometer (IRMS) was used, with a precision of 0.1‰ for  $\delta^{13}\text{C}_{\text{org}}$  and 0.3‰ for  $\delta^{15}\text{N}$ . The

running standard was a protein hydrolysate calibrated against NIST standards. Isotope ratios are expressed in units per mil (‰).

### 3.4 Pigments

Chlorophyll *a* (chl *a*) and phaeopigment (phae) concentrations were estimated fluorometrically from a known amount of freeze-dried sediment (~1 g). Pigments were extracted in 90 % acetone at -20° C for 24 h. After filtration, fluorescence was measured with a digital Turner Designs Model AU10. The fluorometer was calibrated with six dilutions using chlorophyll *a* from SIGMA Co. as standard; concentrations were measured spectrophotometrically (Jeffrey and Humphrey, 1975). These analyses were carried out at the Polar Phytoplankton Laboratory of Scripps Institution of Oceanography, La Jolla, California. Pigment concentrations are reported in µg/g and also normalized to TOC (µg/g TOC). The chl *a*:phae ratio was used as an indicator of chlorophyll preservation, where high values are indicative of good preservation (Sañé et al., 2011).

### 3.5 Sterols

Extraction of total lipids was carried out following Bligh and Dyer (1959), with a slight modification: dichloromethane (DCM) was substituted for chloroform. Freeze-dried sediment samples (*ca.* 3 g) were sequentially extracted by ultra-sonication with 30 mL DCM/methanol (1:3 v/v, 2X), (1:1 v/v, 1X), and DCM (2X). Lipid extracts were concentrated with a rotary evaporator, dried with anhydrous Na<sub>2</sub>SO<sub>4</sub>, and then separated into four fractions by column chromatography (30 cm length, 1 cm ID) filled with *ca.* 7 g of deactivated silica gel. Aliphatic hydrocarbons (F1) were eluted with 40 mL hexane, ketones (F2) with 50 mL toluene/hexane (1:3 v/v), alcohols (F3) with 50 mL ethylacetate/hexane (1:9 v/v), and polar compounds (F4) with 35 mL ethylacetate/methanol/hexane (4:4:1 v/v). The alcohol fraction (F3) containing steroidal biomarkers was derivatized with 80 µL BSTFA (N,O-bis (trimethylsilyl) trifluoroacetamide) and 40 µL TMCS

(trimethylchlorosilane) at 70°C for 1 h before gas chromatography-mass spectrometry analysis, using an Agilent 6890 GC series coupled to an Agilent 5972 MS. Sterols were analyzed with a 30 m DB-5 column (0.5 mmID, 0.25 µm film thickness), using He as a carrier gas. The oven temperature program included 60°C (2 min) to 150°C at 15°C min<sup>-1</sup>, to 320°C (held for 34.5 min) at 4°C min<sup>-1</sup>. The MS was operated in electron impact mode (70 eV) with the ion source at 250°C. Mass spectra were acquired in full scan mode (m/z range 40–600, scan rate 2.6 s<sup>-1</sup>). Sterols were identified through the fragmentation pattern of their trimethylsilyl (TMS) derivatives.

Sterol concentrations were based on the calibration curve made with the external standard cholesterol (Sigma Aldrich Grade, ≥99%) and were normalized to TOC (µg/g TOC) to account for differences in sedimentation rates.

We also calculated Shannon's diversity index (Shannon, 1948) as:

$H' = -\sum_{i=1}^n p_i \ln(p_i)$ , where  $n$  is the total number of sterols and  $p_i$  the proportion of concentration of each compound.

### 3.6 Diatoms

We selected a set of 24 surface sediment samples across the study area for diatom analysis. Samples were treated with hydrogen peroxide (35%) and HCl, and quantitative slides for light microscopy were prepared following the standard procedure developed at AWI (Gersonde and Zielinski, 2000). An average of 560 (minimum 224, maximum 1395) diatom valves was counted per slide using a Zeiss Axioplan II microscope at a magnification of ×1000. The counting procedure followed Schrader and Gersonde (1978).

Diatoms were identified to species or species group level and, if applicable, to a variety or form level following the taxonomy described in Hasle and Syvertsen (1997), Zielinski and Gersonde (1997), and Armand and Zielinski (2001). *Chaetoceros* species (representing mostly resting spores)

were not identified to species level. The two varieties *Eucampia antarctica* var. *antarctica* and *E. antarctica* var. *recta* could not clearly be separated and were combined in the *Eucampia antarctica* group. *Thalassiosira* sp. 3 resembles the resting spore morphological type 1 (*Thalassiosira antarctica* T1) described by Taylor et al. (2001), typically found in sea-ice associated environment.

The preservation state of the diatoms was noted, providing additional information for assessing the robustness of the observed sedimentary distributions, as selective diatom preservation might bias the reference dataset. The preservation stages “good”, “moderate”, and “poor” were distinguished following Esper et al. (2010).

### 3.7 Statistical analyses

A correlation matrix of Spearman was used for a Principal Component Analysis (PCA) on the following 12 variables: diatom abundance (valves/g dry sediment), contents of siliciclastic material, CaCO<sub>3</sub>, biogenic opal, TOC, TN, total pigments and total sterols, molar C/N, stable isotopes  $\delta^{13}\text{C}_{\text{org}}$  and  $\delta^{15}\text{N}$ , and water depth at each sampling site. This analysis was performed with the software Rstudio (R Core Team, 2017). The parameters of a biplot can be directly related to sediment composition and differences in the oceanographic areas to be compared. In this case, the length of the arrow representing a known variable is a function of its importance in determining the parameters' variation. Those that plot close to the center of the diagram show no significant variation within the dataset.

Permutational multivariate analysis of variance (PERMANOVA) was carried out to compare the different oceanographic zones. The adonis function was used for this analysis in RStudio on the logarithm ( $x + 1$ ) of the matrix. PERMANOVA is a resampling technique that allows identifying significant differences in the composition of parameters between groups of samples (stations),

after which it is possible to make comparisons by pairs (zone pairs). Values of  $p < 0.05$  were considered significant.

Additionally, a PCA was performed on the diatom abundance data using the program CANOCO (CANONical Community Ordination: version 4.5 for MS Windows, author C.J.F. Tel' Braak 1992, Wageningen, The Netherlands). Taxa occurring only once within the 24 samples studied and taxa identified to genus level only were excluded from the analysis. *Asteromphalus hookeri* was also removed from the PCA because of its very low abundances (cumulative % in 24 samples  $< 0.4\%$ ). Due to similar ecological preferences reported by Esper et al. (2010, 2014 a,b), we grouped *Azpeitia tabularis* var. *tabularis* and *A. tabularis* var. *egregius* to *A. tabularis* group; *Thalassionema nitzschioides* var. *lanceolata* and *T. nitzschioides* var. *capitulata* to *T. nitzschioides* group, and *Thalassiosira gracilis* var. *gracilis* and *T. gracilis* var. *expecta* to *T. gracilis* group. Thus, 43 diatom taxa remained and were included in the PCA. To enhance the statistical significance of rare species and down rank the significance of the few dominant species, i.e. *Fragilariopsis kerguelensis* and *Chaetoceros* resting spores (CRS), relative abundance data (%) were transformed to logarithm values, using the equation:  $X = \text{LOG}(10 * [\text{relative abundance}] + 1)$ .

The PCA is based on the assumption that diatom species show a linear response to changing environmental gradients, i.e. increase or decrease in abundance linearly along an increasing environmental gradient such as temperature. In the PCA, species are arranged along hypothetical axes in such a way that the first axis (or x-axis) represents a gradient (or a combination of gradients) which causes the largest variation in species composition; the second axis (or y-axis) represents the second most important direction of variation, etc. The gradients determining the species variance can be biotic or abiotic.

#### 4. Results

#### 4.1 Bulk sediment composition

The bulk composition of the surface sediments varied latitudinally and showed the highest contents of biogenic opal (8–19%) and siliciclastic material (75–89%) in the BS and SSI, whereas carbonate dominated in the SAZ (45–71%; Fig. 2). Exceptions occurred at two sites located at relatively shallow depths on the Hero Fracture Zone south of the PF (PS97/045 and PS97/044, Table S1); these sites yielded  $\geq 90\%$   $\text{CaCO}_3$  (Table S1). The relative concentrations of TOC and TN increased southward, reaching peak values of  $\sim 1\%$  and  $\sim 0.17\%$ , respectively, in the SSI-BS area (Table S1). C/N values ranged 4.7–11.9, with lower values at the continental Chilean/Argentinian margin sites and higher values south of the SACCF (Fig. 3a). The notably higher C/N values in the Hero Fracture Zone (11.1 and 11.9) occurred at sites PS97/044 and PS97/045 (mentioned above), where extremely high  $\text{CaCO}_3$  and low TOC contents were found (Table S1).

#### 4.2 Stable isotopes

Surface sediments of the study area displayed a wide range of  $\delta^{13}\text{C}_{\text{org}}$  values (Fig. 3b), varying between  $-25.74$  and  $-19.13$  ‰. The highest values corresponded to sediments along the Chilean continental margin, whereas lower values occurred south of the PF (Fig. 3b). Values of  $\delta^{15}\text{N}$  were in the range of 2.6 to 6.2 ‰ and were lowest at sites PS97/089 and PS97/086 close to the PF (Fig. 3c, Table S1).

#### 4.3 Pigments

The abundance of total photosynthetic pigments preserved in the surface sediments increased from the coast of Chile towards Antarctica, with minimum values in the DP (Fig. 4; normalized and non-normalized data are given in Table S1). On average for the entire study area, the concentration of total pigments was  $2062.6 \pm 3324.6$   $\mu\text{g/g}$  TOC (phaeopigments  $1859.7 \pm$

3016.0  $\mu\text{g/g}$  TOC and chl *a*  $209.3 \pm 332.7$   $\mu\text{g/g}$  TOC). Total pigment spatial distribution was patchy, especially south of the SACCF, from an extremely low value northwest of Elephant Island (station PS97/077: 92.5  $\mu\text{g/g}$  TOC at 3586 m water depth) to the highest values offshore Nelson Island (station PS97/067: 12878.3  $\mu\text{g/g}$  TOC at 550 m water depth) and in Maxwell Bay (PS97/071: 12194.3  $\mu\text{g/g}$  TOC at 441 m water depth) (Table S1, Fig. 4). Low values were also found on the Chilean margin and in the western section of the DP (Fig. 4b).

Phaeopigments dominated the sediment pigment inventory with concentrations being one to two orders of magnitude higher than chl *a* values (Table S1, Fig. 4d). In fact, poor chl *a* preservation was observed over the entire study area, with chl *a*:phae ratios of 0.004–0.31 (Table S1). No clear latitudinal pattern could be discerned, although our findings point to somewhat better preservation of chl *a* in the PFZ (PS97/084, 085 and 086) and within the BS (site PS97/056; Table S1).

#### 4.4 Sterols

Total sterol concentrations were lowest in the DP ( $263.3 \pm 95.1$   $\mu\text{g/g}$  TOC), somewhat higher and very variable along the Chilean/Argentinian margin ( $382.8 \pm 209.7$   $\mu\text{g/g}$  TOC), and highest in the SSI ( $2197.8 \pm 1380.2$   $\mu\text{g/g}$  TOC). The total range in the study area was 78.0 to 4363.4  $\mu\text{g/g}$  TOC (Fig. 4e; normalized and non-normalized data are given in Table S1). We identified 13 sterols (Fig. 5, Table S2), including: (1)  $\text{C}_{26}$ -sterols: 22,24-cyclocholest-5-en (propil  $\text{C}_{26}\Delta^5$ ), 24-nor-5 $\alpha$ -cholest-22-en-3 $\beta$ -ol ( $\text{C}_{26}\Delta^{22}$ ); (2)  $\text{C}_{27}$ -sterols: cholest-5-en-3 $\beta$ -ol ( $\text{C}_{27}\Delta^5$ , Cholesterol), 5 $\alpha$ -cholestan-3 $\beta$ -ol ( $\text{C}_{27}\Delta^0$ , Cholestanol), cholesta-5,24-dien-3 $\beta$ -ol ( $\text{C}_{27}\Delta^{5,24}$ , Desmosterol), and cholest-4-en-3-one ( $\text{C}_{27}\Delta^4$ , Cholestenone); (3)  $\text{C}_{28}$ -sterols: 24-methylcholest-5,22E-dien-3 $\beta$ -ol ( $\text{C}_{28}\Delta^{5,22}$ , Brassicasterol), 24-methylcholesta-5,24(28)-dien-3 $\beta$ -ol ( $\text{C}_{28}\Delta^{5,24(28)}$ , methylenecholesterol), 24-methylcholest-5-en-3 $\beta$ -ol ( $\text{C}_{28}\Delta^5$ , Campesterol), and stigmata-5,24(28)-dien-3 $\beta$ -ol ( $\text{C}_{28}\Delta^{5,24}$ , Fucosterol); (4)  $\text{C}_{29}$ -sterols: 24

ethylcholest-5,22E-3 $\beta$ -ol (C<sub>29</sub> $\Delta^{5,22}$ , Stigmasterol); 24-ethylcholest-5-en3 $\beta$ -ol (C<sub>29</sub> $\Delta^5$ ,  $\beta$ -sitosterol); and (5) C<sub>30</sub>-sterols: 4 $\alpha$ ,22,23-trimethylcholest-22E-en-3 $\beta$ -ol (C<sub>30</sub> $\Delta^{22}$ , Dinosterol). Possible sources of these sterols are given in Table 1.

Overall, sterol diversity ( $H'$ ) was low (0.62–0.72); relatively higher and rather constant values were found south of the PF and more variable values in subantarctic waters. Lowest diversity occurred at offshore stations PS97/114, PS97/093, and PS97/094 and at the continental margin stations PS97/024, 095 and 096 (Fig. 5). Cholesterol was the dominant sterol component detected in practically the entire study area representing, on average, 34% of the total sterols (total abundance range: 14–1835  $\mu\text{g/g}$  TOC). An exception was station PS97/086 on the PF, where cholesterol accounted for only 3% of total sterols (Fig. 5, Table S2). Desmosterol (14–584  $\mu\text{g/g}$  TOC) was found exclusively in the SSI-BS area. Third in absolute abundance was  $\beta$ -sitosterol (14–544  $\mu\text{g/g}$  TOC), with the highest values in the SSI area (avg. 249  $\mu\text{g/g}$  TOC) and moderately high along the Chilean/Argentinian continental margins (avg. 108  $\mu\text{g/g}$  TOC); relative abundance of this sterol was highest at the low diversity stations PS97/095 and 096. Concentrations of stigmasterol (7.5–259  $\mu\text{g/g}$  TOC) were also highest in the SSI area. Campesterol (2.8–151  $\mu\text{g/g}$  TOC) was only observed at Chilean continental margin sites and in the sSIZ where it reached a maximum value at station PS97/056 (Table S2). Brassicasterol was present in practically the entire study area (11–274  $\mu\text{g/g}$  TOC), with peak concentrations at SSI-BS stations (Table S2). Dinosterol abundance reached >75  $\mu\text{g/g}$  TOC at SSI stations and was absent from SAZ offshore samples and most of the western DP sites. Methylenecholesterol was measured along the Chilean margin and south of the SACCF. The occurrence of fucosterol was very sporadic in the SAZ and in the DP, whereas it was regularly present in the SSI-BS area with peak concentration at station PS97/067 (166  $\mu\text{g/g}$  TOC; Table S2).

#### 4.5 Diatom abundance and species distribution pattern

The concentration of diatoms in surface sediments varied between  $1.2 \times 10^6$  and  $112.2 \times 10^6$  valves/g dry sediment, and an overall N-S pattern from lower to higher concentrations was seen (Fig. 6, Table S3): average  $4.5 \times 10^6$  valves/g in the SAZ,  $20.9 \times 10^6$  valves/g in the PFZ+POOZ, and  $44.8 \times 10^6$  valves/g in the Antarctic Peninsula area. This pattern was mirrored by the content of sedimentary biogenic opal (Fig. 2c); the correlation between both variables was positive and significant ( $r= 0.75$ ,  $p<0.001$ ; Table 3). Diatoms were moderately preserved (Fig. 6) except at stations PS97/114, PS97/094, PS97/052, PS97/069, and PS97/072 (moderate to poor preservation) and stations PS97/071 and PS97/073 (good to moderate preservation; Fig. 6, Table S3).

A total of 53 diatom taxa were identified and counted (Table 2; relative abundances in Table S3). To investigate the relationship between diatom assemblage composition and oceanographic regions in the study area, a PCA of the 24 selected sediment surface samples and 42 diatom taxa was performed (Fig. 7). The PCA explains 71% of variance with the first four principal components (PC1: 44.9%, PC2: 13.5%, PC3: 7.6%, PC4: 5.1%; Tables S4 and S5). PC1 resembles an indirect gradient most likely associated with variation in sea surface temperature/sea-ice cover, with cold water/sea-ice related taxa in the sSIZ (e.g., *Actinocyclus actinochilus*, *Fragilariopsis curta*, *F. cylindrus*, *Odontella weissflogii* and *Chaetoceros* resting spores) plotting to the right-hand side (positive PC1-values). Warmer water related taxa in the SAZ (e.g., *Azpeitia tabularis*, *Eucampia antarctica*, *Roperia tessellata* and *Thalassionema nitzschioides*), on the other hand, plot to the left-hand side (negative PC1-values). PC2 is associated with taxa representing the transitional zone (TZ) of the Antarctic Peninsula continental margin (*Fragilariopsis separanda* and *Thalassiosira gracilis*) between the sSIZ and the PFZ+POOZ (Fig. 7a), the latter is dominated by the coarsely silicified species *Fragilariopsis kerguelensis* and accompanied by *Thalassiosira lentiginosa*. The two-dimensional distribution of the 24 samples within the PC1/PC2-space clearly reflects a regional character of the diatom assemblage composition. Samples dominated by taxa associated with the

sSIZ plot to the right-hand side of PC1, taxa characterizing the SAZ assemblage plot to the left-hand side of PC1. Negative values of PC2 are associated with assemblages from the PFZ+POOZ area, with a clear distinction of the 3 stations representing the TZ (Fig. 7b).

#### 4.6 Geochemical-environment relationships

The PCA of the 12 variables measured in the 51 surface samples revealed two main axes that explain 58.3% of the total variance (Fig. 8; Table S6). The first component (PC1) accounted for 44% of the total variance. The variables with the highest positive loadings were biogenic opal (1.19), TOC (1.19), sterols (1.15), TN (1.14), and siliciclastics (1.03) and plot on the right-hand side of PC1. Negative loadings correspond to  $\text{CaCO}_3$  (-1.12) and  $\delta^{13}\text{C}_{\text{org}}$  (-0.71) (Fig. 8). The second component (PC2) explained 14% of the variance, with the highest positive loadings for depth (0.90) and siliciclastic content (0.79) and negative loadings for  $\text{CaCO}_3$  (-0.74) and  $\delta^{13}\text{C}_{\text{org}}$  (-0.68) (Fig. 8). All variables showed significant correlations (Table 3). Almost all continental margin samples and/or those shallower than 2,500 m fell on negative values of the PC2 axis, whereas the deeper stations grouped on positive values (Fig. 8).

Based on the parameters measured, the PERMANOVA analysis indicated significant differences among the biogeographical zones (SAF, PFZ+POOZ, TZ and sSIZ): PERMANOVA global:  $p < 0.05$  and PERMANOVA pairwise:  $p < 0.05$ .

## 5. Discussion

Our multi-proxy approach documents the N-S spatial variability in the composition of surface sediments across the entire DP. The organic and inorganic proxies and the diatom species preserved in the surface sediments of the study area revealed large spatial variability that seems

to be associated with sea surface temperature gradients, organic matter pulses to the sea floor, intensity of currents, proximity to ice, and terrigenous input, clearly differentiating among biogeographical zones (Figs. 7 and 8).

In the following sections, we discuss each of the proxies analyzed herein, and compare them with published work.

### *5.1 Variations in sediment composition*

A contrasting trend is seen in the distribution of biogenic opal vs.  $\text{CaCO}_3$  contents ( $r=-0.79$ ,  $p<0.001$ , Table 3), with biogenic opal being most important in the TZ and sSIZ and close to the SACCF in the central DP (>8%) whereas  $\text{CaCO}_3$  dominates in the SAZ ( $\geq 45\%$ ) and at the topographic rise in the western DP (Fig. 2; Table S1). The geochemical results agree with the microscopic characterization of the sediments done onboard R/V Polarstern (smear-slide and coarse fraction analyses; Lamy, 2016), which revealed nannofossil/foraminifer-rich sediments north of the SAF and diatom-rich sediments in the Antarctic Peninsula area. The general N-S transition from carbonate-rich to opal-rich sediment has long been recognized in water column, sediment trap, and surface sediment studies in the SO (e.g., Honjo et al., 2000; Pondaven et al., 2000; Nelson et al., 2002; Ragueneau et al., 2002; Honjo, 2004; Geibert et al., 2005; Chase et al., 2015; Rigual-Hernández et al., 2015). The overall lower opal content in the SAZ is in agreement with the depletion of silicate in surface waters (e.g., DiTullio et al., 2003; Sarmiento et al., 2004; Chase et al., 2015).

An interesting result was obtained from the initial sediment analysis of the coarse fraction (>63  $\mu\text{m}$ ) done onboard, which showed foraminifera-rich sediments south of the PF, in particular along the western DP transect (H. Schulz, pers. comm.). This observation would extend the so-called foraminifera belt described earlier on material from the Eltanin expedition further south

(Goodell, 1964, 1965, Herb, 1968). A shallower sample depth (PS97 sites mostly shallower than Herb's at the same/similar latitude and longitude) and the use of coring equipment during PS97 that retrieved an intact sediment/water interface may have been the factors responsible for a better preservation of PS97-sourced calcareous sediments.

The spatial distribution of TOC in the surface sediments follows that of biogenic opal ( $r=0.68$ ,  $p<0.001$ ) and diatoms ( $r=0.71$ ,  $p<0.001$ ), and TN follows the pattern of TOC ( $r=0.98$ ,  $p<0.001$ , Table 3). For the Antarctic Peninsula area, our TOC values (average: 0.75%, Table S1) are comparable to those given by Isla et al. (2004) for the Gerlache Strait and BS, and Isla (2016) and Veit-Köhler et al. (2018) for the BS and around the SSI.

Overall, low molar C/N (average: 6.7, range: 4.7–8.9) and stable carbon isotope values of 23.8‰ ( $\delta^{13}\text{C}_{\text{org}}$  range: -25.7 to -19.1‰) in most of the surface sediments point to a predominance of marine-derived organic matter in our study area. C/N values in the sSIZ are on the “higher end” of our range (Table S1, Fig. 3a) and are similar to published ones for sediment traps and surface sediments in this area (Masqué et al., 2002; Palanques et al., 2002; Isla et al., 2004; Veit-Köhler et al., 2018). With respect to  $\delta^{13}\text{C}_{\text{org}}$ , a change from heavier to lighter values happens near the PF (Table S1, Fig. 3b; roughly along the transition from carbonate to opal sediments) and values in the range of -24.1 to -25.7‰ (characteristic of Antarctic plankton, Venkatesan & Kaplan, 1987) are observed at our Antarctic Peninsula sites. Mincks et al. (2008) and Learman et al. (2016) reported similar surface sediment values (-24.0 to -25.9‰ around Anvers Island, and -23.5 to -24.6‰ along the Peninsula coast and in the BS, respectively). The study by Popp et al. (1999) has demonstrated that across the Southern Ocean, availability of  $\text{CO}_2(\text{aq})$  and changes in algal assemblage composition are key drivers of carbon isotopic composition of suspended particulate organic matter. Also, while our slightly higher C/N values in the Antarctic Peninsula area could relate to the transport and deposition of reworked/eroded terrigenous material by means of ice-rafting or

supply of sediment-laden meltwater plumes to the bays of the SSI (Hass et al., 2010), the lower  $\delta^{13}\text{C}_{\text{org}}$  values in these sediments may be attributed to other/additional factors. For example, a change in assemblage composition or the utilization of carbon-concentrating mechanisms in different algae (Giordano et al., 2005) or lack of this biochemical mechanism (as in the diatom *Proboscia inermis*), as well as the presence of sea ice have been shown to impact the  $\delta^{13}\text{C}_{\text{org}}$  signature preserved in coastal Antarctic environments (e.g., Cassar et al., 2004; Henley et al., 2012).

## 5.2 Preservation of sedimentary pigments and sterols

Pigments and other biomarkers preserved in sedimentary records have been widely used in reconstruction studies of primary production, organic carbon transfer to the sediments, sources of organic matter, and environmental conditions (e.g., Gagosian et al., 1980; Sauer et al., 2001; Ceschim et al., 2016; Dauner et al., 2017). Bulk organic carbon degradation studies have shown dramatic changes in the composition of organic matter with water column depth and at the sediment-water interface, as well as preferential degradation of the more labile components, i.e., pigments are more labile than sterols (Wakeham et al., 1997; Lee et al., 2000).

Chlorophyll *a* is produced in the photic zone and is commonly used to estimate phytoplankton biomass in the water column (Mantoura and Llewellyn, 1983; Sun et al., 1994). Its presence in sediments correlates with organic carbon from phytoplankton origins and, thus, can be considered as a useful proxy of primary production in the water column (Sun et al., 1991; Villanueva and Hasting, 2000). Phaeopigments, on the other hand, relate to early diagenetic processes of chlorophyll (e.g., Mantoura and Llewellyn, 1983) and are usually found in zooplankton and protozoan fecal pellets (Harris et al., 1995). The conversion of chl *a* to phaeopigments is fast and only chl *a* derivatives (i.e., phaeopigments) are found in non-living

phytoplankton cells (Vernet and Lorenzen, 1987). Unlike photosynthetic pigments, sterols are not limited to the euphotic zone and derive from different biological sources (Gagosian et al., 1980; Volkman, 2003).

Our results yielded a marked N-S pattern, with peak pigment concentrations around SSI and in the BS (Fig 4, Table S1), which we consider to be a reflection of the large phytoplankton blooms that develop during the summer in the Antarctic Peninsula (Holm-Hansen and Mitchell, 1991; Basterretxea and Arístegui, 1999; Rozema et al., 2017; Aracena et al., 2018) and their export to the seafloor. Our findings support the general basin-wide pattern in which chl *a* and derivatives are associated with carbon content (%) in sediments, decrease in concentration with water-column depth (Fig. 4, Table 3), and with fine silt (Table S1; Szymczak-Zyła et al., 2011). The concentration of total sterols follows the same pattern as the pigments (Fig. 4; Table S1) with highest values in the SSI and the BS (as high as 4636 µg/g TOC at station PS97/067, Fig. 4e), which again can be associated with the high export and accumulation of organic matter in the area (Isla, 2016).

As stated above, the concentration of phaeopigments in the surface sediments of the study area was at least an order of magnitude higher than chl *a* concentrations, and high variability characterized both pigments ( $9.8 \pm 16.4$  µg/g and  $1.2 \pm 2.1$  µg/g, respectively; Table S1). Similar concentrations were also found by Sañé et al. (2011) and Veit-Köhler et al. (2018) in sediments of the BS and the northeastern tip of the Peninsula, ranging from 0.15 to 18.73 µg/g, and suggesting high and consistent input of phytoplankton carbon to the seafloor. However, the overall low levels of chl *a* preservation in the study area (chl *a*:phae of  $0.1 \pm 0.07$ , Table S1) might be related to its fast degradation in the water column by photo-oxidation at the surface and grazing throughout the water column; degradation continues at the sediment-water interface, where oxic conditions may accelerate the process (Leavitt, 1993; Sun et al., 1993; Leavitt and Hudgson, 2001). Published chl *a*:phae data in surface sediments are mostly limited to the Antarctic Peninsula region. Here,

our values are similar to the ones given by Sañé et al. (2011) for surface sediments offshore SSI and from Elephant Island (~0.1), for sediment traps in Deception Island (~0.2; Baldwin and Smith, 2003) and Anvers Island (~0.3; Smith et al., 2008), but are much lower than the ones reported for the BS (~2.2; Veit-Köhler et al., 2018). Whether this difference in degradation index values is associated with lower bioturbation that allows for better chl *a* preservation (Bianchi et al., 2000) cannot be ascertained at this time.

The elevated TOC, pigments and sterols in the vicinity of the Antarctic Peninsula are related to several factors, including seasonal organic matter pulses (Isla, 2016; Veit-Köhler et al., 2018), high accumulation rates (Harden et al., 1992), sluggish currents in inshore waters of the SSI, and/or focusing effect and development of depocenters in the BS (e.g., Ichii et al., 1998; Isla et al., 2004; Zhou et al., 2006). In contrast, the low values north of the SACCF in the DP (Table S1) could be associated with both water column depth (most sites at >3,000 m) and strong bottom currents winnowing the sediments (Heezen and Hollister, 1964). Near-bottom velocities >30 cm/s at the SAF and ~20 cm/s at the PF have been reported by Provost et al. (2011). Preliminary L-ADCP data from the PS97 cruise yielded near-bottom velocities of ~15 cm/s for the PF (H. Fenco, pers. comm.), which are similar to the speeds reported by Donohue et al. (2016) for the central DP at the Shackleton Fracture Zone.

#### 5.2.1 Sources of sterols

The relative contribution of distinct sterols (Fig. 5) indicates the existence of multiple sources of sedimentary organic matter, i.e., terrestrial plants, marine phytoplankton and zooplankton, macroalgae, soils, and fungi (Table 1; e.g., Volkman, 1986, 2003).

The most abundant sterol in the study area is cholesterol, which is traditionally related to zooplankton (Volkman, 1986). Because other source organisms have been proposed for

cholesterol, its use in sediments as a tracer for a particular source could be questioned (Volkman, 1986, 2003; Volkman et al., 1993). For example, Nelson et al. (2001) reported this sterol as the most abundant in Cnidaria off the Antarctic Peninsula, krill species, and Antarctic salps and amphipods (Phleger et al., 2000). Desmosterol was only detected in the sSIZ (Table S2), an area characterized by cold water diatom species (Table S3, Fig. 7). These findings support Rampen et al. (2010), who associated desmosterol with sea-ice-related centric diatoms such as *Corethron pennatum*, *Actinocyclus actinochilus* and *Stellarima microtrias*. Desmosterol has also been reported as an important sterol in krill (Phleger et al., 1998) and Antarctic amphipods (Nelson et al., 2001).

The concentrations of brassicasterol, a common sterol in diatoms and *Phaeocystis* (Volkman, 1986; Villinski et al., 2008), and dinosterol, an abundant sterol in dinoflagellates (Volkman, 2003) in almost all samples (Table S2) fall within the range reported by Wisnieski et al. (2014) for sediments of Admiralty Bay, and Ceschim et al. (2016) for Penguin Island. Brassicasterol is also abundant in haptophytes and cryptophytes (Goad et al., 1983; Volkman, 1986) and its ubiquitous occurrence in the study area points to a multiple sourced origin. Dinosterol was not detected in 10 samples from the DP, which, however, should not be interpreted as indicative of the absence of dinoflagellates as dinosterol is also found in some diatoms (*Navicula*, Volkman et al., 1993). We consider that low sedimentation rates at these distal marine sites account for the absence of dinosterol (and other sterols with generally low concentrations; e.g. cholestenone).

The distribution of fucosterol, a major sterol in macroscopic brown algae (e.g., Volkman, 1986; Pereira et al., 2017), was mainly restricted to SSI stations. This is not surprising since large phaeophytes have been reported for the South Orkney Islands, the SSI, and the northern part of the Antarctic Peninsula (Klöser et al., 1996).

The sterols  $\beta$ -sitosterol, stigmasterol, and campesterol are common in epicuticular waxes of vascular plants (e.g., Volkman, 1986, 2003; Rontani et al., 2014). Their contribution along the Chilean/Argentinian continental margin (Fig. 5) may be attributed to subantarctic deciduous beech (*Nothofagus* spp.) and evergreen beech forests (*N. betuloides*, *Drimys winteri*) that cover Patagonia (Malainey et al., 2015). For the Drake Passage and the Antarctic Peninsula and adjacent islands, however,  $\beta$ -sitosterol and stigmasterol may be associated with a marine source (i.e., the presence of macroalgae; Volkman, 1986); eolian transport cannot be ruled out but data are not sufficient to assure/reject this source. Campesterol, instead, seems to be more reliable in reflecting a terrestrial signal as it seems to be confined to near-coastal and continental shelf areas.

### 5.3 Distribution of diatoms

The distribution of diatoms in surface sediments of the SO has been studied by several authors, revealing clear patterns that can be related to surface water properties (e.g., Zielinski and Gersonde, 1997; Armand et al., 2005; Crosta et al., 2005; Romero et al., 2005; Esper et al., 2010; Esper and Gersonde, 2014b), despite the many processes that can alter the living assemblage during sedimentation and accumulation, resulting in a modified sedimentary assemblage. Our study shows diatom concentrations following a clear latitudinal pattern, with increasing values at and south of the PF in the “opal belt” and in the BS, consistent with the distribution of biogenic opal content (Figs. 2c, 6, Table S1). The species distribution reflects dependency on the frontal systems of the ACC and its related temperature zonation (Fig. 7). Our observations are in general agreement with previous studies in the Atlantic and eastern and central Pacific sectors of the SO (Zielinski and Gersonde, 1997; Esper et al., 2010; Esper and Gersonde, 2014 a,b).

Although sampling coverage is sparse in the SAZ, a distinct assemblage of warmer-water diatoms characterizes the northern DP sediments and the Chilean/Argentinian margin (Table S3,

Fig. 7). This assemblage thrives in water temperatures of 4–14°C (Esper and Gersonde, 2014a) and is limited to the south by the SAF. Its distribution pattern is in accordance with previous diatom studies from the southeastern Pacific sector of the SO (Esper et al., 2010), the subantarctic Atlantic (Romero et al., 2005), and Australian sectors (sediment traps; Rigual-Hernandez et al., 2014). Drake Passage sediments of the PFZ+POOZ are dominated by *Fragilariopsis kerguelensis* (60–77%), matching observations by Esper et al. (2010) and Crosta et al. (2005). The high contribution of this robust species is related to preservation efficiency (Pichon et al., 1992; Esper et al., 2010). The assemblage is moderately preserved in the PFZ+POOZ, also extending its distribution into the SAZ (Table S3); it is restricted to a temperature range between -1 and 4°C (Esper and Gersonde, 2014b). A transitional assemblage of the Antarctic continental margin separates from the PFZ+POOZ to the north and the sSIZ to the south (Fig. 7). The assemblage in the SSI-BS area is restricted to sea surface temperatures below 0 °C (Esper and Gersonde, 2014a); the high concentrations in the sSIZ indicates a strong relationship to sea ice occurrence (Table S3). Its distribution pattern agrees with sediment trap and surface sediment observations by Leventer (1991, 1992), Esper et al. (2010), and Armand et al. (2005). In the BS sediments, *Chaetoceros* spp. resting spores dominate the diatom assemblage accounting for, on average, ~77% (Table S3), in accordance with data previously reported by Gersonde and Wefer (1987). The absolute abundance of these spores in the sediments reaches up to  $86 \times 10^6$  spores/g, a value that is one order of magnitude lower than the data by Crosta et al. (1997) from the Gerlache Strait. The high occurrence of *Chaetoceros* resting spores in nearshore sediments of the Antarctic Peninsula and the BS has been related to spring/summer blooms caused by meltwater-induced surface stratification in the vicinity of retracting sea ice (e.g., Crosta et al., 1997; Esper et al., 2010; Świło et al., 2016).

## 6. Conclusions

Our multi-proxy approach documents the spatial variability in the composition of surface sediment samples across the DP from the Chilean/Argentinian continental margin to the Antarctic Peninsula area. Based on inorganic and organic parameters studied, a principal component analysis (PCA) clearly differentiated two zones with contrasting characteristics: the SAZ (at and to the north of the SAF) with high  $\text{CaCO}_3$  and low contents of TOC, pigments and sterols, whereas high TOC, pigments, and sterols as well as peak diatom abundances describe the sediments of the SSI-BS area in the sSIZ. The PCA also captured the variability in water depth, differentiating shallower from deeper sites. C/N and stable carbon isotope values point to a predominance of marine-derived organic matter in our study area. An overall low chl  $a$ :phae ratio suggests phytoplankton carbon has been degraded through grazing and other diagenetic processes before reaching the sediments.

Thirteen sterols were detected in the study area. Cholesterol was the most abundant sterol followed by desmosterol, which was only detected in the sSIZ, in coincidence with the diatom assemblage generally associated with sea-ice. The ubiquitous presence of  $\beta$ -sitosterol in near-coastal as well as distal marine sites suggests either an additional algal source of this lipid or eolian transport.

Diatom concentrations at and south of the PF were generally one order of magnitude higher than north of it. Biogenic opal and diatom abundance were highly correlated. Diatom species grouped in 4 assemblages characterizing the SAZ, PFZ+POOZ, TZ and sSIZ; their distribution clearly reflects the N-S environmental gradients of sea surface temperature and sea ice extent.

In conclusion, the biogeochemical and diatom composition of the surface sediments in the DP varies latitudinally according to oceanographic conditions. The new data set presented here

represents a useful regional baseline for future paleo-reconstructions in a rapidly changing environment and with highly variable oceanographic characteristics.

### **Acknowledgements**

We thank Captain Schwarze and his crew on the RV Polarstern, for a successful PS97 cruise. We are grateful to D. Nürnberg and the members of the PS97 Geology Science Party for endless hours of site surveys, coring, sub-sampling and initial sediment analysis onboard. We thank L. Rebolledo (INACH, Punta Arenas, Chile) and H. Schulz (Universität Tübingen, Germany) for sub-sampling of MUCs, smear-slides and coarse fraction analyses carried out on Polarstern. H. Fenco (INDEP, Mar del Plata, Argentina) provided preliminary analysis and interpretation of ACC current velocities. We acknowledge laboratory assistance by V. Acuña and A. Ávila (Universidad de Concepción, Chile) for sterols and biogenic opal measurements, B.J. Pan and L. Ekern (Scripps Institution of Oceanography, USA) for pigments analyses, and S. García (Universidad de Concepción, Chile) for help in the preparation of Figures 1 and 2. This work benefitted from fruitful discussions with J.L. Iriarte (UACH, Puerto Montt) and H. Schulz.

We thank the Alfred-Wegener Institut, Helmholtz Zentrum für Polar and Meeresforschung for funding Polarstern expedition PS97. We acknowledge financial support from the Center for Oceanographic Research COPAS Sur-Austral (CONICYT PIA PFB31 and AFB170006) and the Research Center Dynamics of High Latitude Marine Ecosystems (FONDAP-IDEAL 15150003) (to PC, CBL and BS), Helmholtz Research Grant VH-NG-1101 (to JM and M-EV), research program PACES II: Polar Regions and Coasts in the changing Earth System (to GK, FL), and from the US National Science Foundation (award PLR-1443705 to MV). PC received a scholarship from CONICYT-PFCHA/MagisterNacional/2017-22171017.

## References

- Amante, C., Eakins, B.W., 2009. ETOPO11 arc-minute global relief model: procedures, data sources and analysis. NOAA Technical Memorandum NESDIS NGDC-24. 19 pp.  
<https://doi.org/10.7289/V5C8276M>
- Anderson, R.F., Chase, Z., Fleisher, M.Q., Sachs, J., 2002. The Southern Ocean's biological pump during the Last Glacial Maximum. *Deep. Res. Part II Top. Stud. Oceanogr.* 49, 1909–1938.  
[https://doi.org/10.1016/S0967-0645\(02\)00018-8](https://doi.org/10.1016/S0967-0645(02)00018-8)
- Anderson, R.F., Ali, S., Bradtmiller, L.I., Nielsen, S.H.H., Fleisher, M.Q., Anderson, B.E., Burckle, L.H., 2009. Rise in Atmospheric CO<sub>2</sub>. *Science* 323, 1443–1448.  
<https://doi.org/10.1126/science.1167441>
- Aracena, C., González, H.E., Vargas, J.G., Lange, C.B., Pantoja, S., Muñoz, F., Teca, E., Tejos, E., 2018. Influence of summer conditions on surface water properties and phytoplankton productivity in embayments of the South Shetland Islands. *Polar Biol.*  
<https://doi.org/10.1007/s00300-018-2338-x>
- Ardelan, M. V., Holm-Hansen, O., Hewes, C.D., Reiss, C.S., Silva, N.S., Dulaiova, H., Steinnes, E., Sakshaug, E., 2010. Natural iron enrichment around the Antarctic Peninsula in the Southern Ocean. *Biogeosciences* 6, 7481–7515. <https://doi.org/10.5194/bgd-6-7481-2009>
- Armand, L.K., Crosta, X., Romero, O., Pichon, J.J., 2005. The biogeography of major diatom taxa in Southern Ocean sediments: 1. Sea ice related species. *Palaeogeogr. Palaeoclimatol. Palaeoecol.* 223, 93–126. <https://doi.org/10.1016/j.palaeo.2005.02.015>
- Armand, L.K., Zielinski, U., 2001. Diatom species of the genus *Rhizosolenia* from Southern Ocean sediments: Distribution and taxonomic notes. *Diatom Res.* 16, 259–294.

<https://doi.org/10.1080/0269249X.2001.9705520>

Baldwin, R.J., Smith, K.L., 2003. Temporal dynamics of particulate matter fluxes and sediment community response in Port Foster, Deception Island, Antarctica. *Deep. Res. Part II Top. Stud. Oceanogr.* 50, 1707–1725. [https://doi.org/10.1016/S0967-0645\(03\)00089-4](https://doi.org/10.1016/S0967-0645(03)00089-4)

Barré, N., Provost, C., Renault, A., Sennéchaël, N., 2011. Fronts, meanders and eddies in Drake Passage during the ANT-XXIII/3 cruise in January-February 2006: A satellite perspective. *Deep. Res. Part II Top. Stud. Oceanogr.* 58, 2533–2554. <https://doi.org/10.1016/j.dsr2.2011.01.003>

Basterretxea, G., Arístegui, J., 1999. Phytoplankton biomass and production during late austral spring (1991) and summer (1993) in the Bransfield Strait. *Polar Biol.* 21, 11–22. <https://doi.org/10.1007/s003000050328>

Beal, L.M., De Ruijter, W.P.M., Biastoch, A., Zahn, R., Cronin, M., Hermes, J., Lutjeharms, J., Quartly, G., Tozuka, T., Baker-Yeboah, S., Bornman, T., Cipollini, P., Dijkstra, H., Hall, I., Park, W., Peeters, F., Penven, P., Ridderinkhof, H., Zinke, J., 2011. On the role of the Agulhas system in ocean circulation and climate. *Nature* 472, 429–436. <https://doi.org/10.1038/nature09983>

Bianchi, T.S., Johansson, B., Elmgren, R., 2000. Breakdown of phytoplankton pigments in Baltic sediments: Effects of anoxia and loss of deposit-feeding macrofauna. *J. Exp. Mar. Bio. Ecol.* 251, 161–183. [https://doi.org/10.1016/S0022-0981\(00\)00212-4](https://doi.org/10.1016/S0022-0981(00)00212-4)

Bligh, E.G., Dyer, W.J., 1959. A rapid method of total lipid extraction and purification. *Can. J. Biochem. Physiol.* 37, 910–917. <https://doi.org/10.1139/o59-099>

Caniupán, M., Lamy, F., Lange, C.B., Kaiser, J., Arz, H., Kilian, R., Baeza Urrea, O., Aracena, C.,

- Hebbeln, D., Kissel, C., Laj, C., Mollenhauer, G., Tiedemann, R., 2011. Millennial-scale sea surface temperature and Patagonian Ice Sheet changes off southernmost Chile (53°S) over the past ~60 kyr. *Paleoceanography* 26, 1–10. <https://doi.org/10.1029/2010PA002049>
- Carter, L., McCave, I.N., Williams, M.J.M., 2009. Circulation and water masses of the Southern Ocean: A Review, in: *Developments in Earth and Environmental Sciences*. pp. 85–114. [https://doi.org/10.1016/S1571-9197\(08\)00004-9](https://doi.org/10.1016/S1571-9197(08)00004-9)
- Cassar, N., Laws, E.A., Bidigare, R.R., Popp, B.N., 2004. Bicarbonate uptake by Southern Ocean phytoplankton. *Global Biogeochem. Cycles* 18, GB2003. <https://doi.org/10.1029/2003GB002116>
- Ceschim, L.M.M., Dauner, A.L.L., Montone, R.C., Figueira, R.C.L., Martins, C.C., 2016. Depositional history of sedimentary sterols around Penguin Island, Antarctica. *Antarct. Sci.* 28, 443–454. <https://doi.org/10.1017/S0954102016000274>
- Chaigneau, A., Pizarro, O., 2005. Surface circulation and fronts of the South Pacific Ocean, east of 120°W. *Geophys. Res. Lett.* 32, 1–4. <https://doi.org/10.1029/2004GL022070>
- Chase, Z., Kohfeld, K.E., Matsumoto, K., 2015. Controls on biogenic silica burial in the Southern Ocean. *Global Biogeochem. Cycles* 29, 1–19. <https://doi.org/10.1002/2014GB004979>
- Chereskin, T.K., Tarling, G.A., 2007. Interannual to diurnal variability in the near-surface scattering layer in Drake Passage. *ICES J. Mar. Sci.* 64, 1617–1626. <https://doi.org/10.1093/icesjms/fsm138>
- Coale, K.H., 2004. Southern Ocean iron enrichment experiment: carbon cycling in high- and low-Si waters. *Science* 304, 408–414. <https://doi.org/10.1126/science.1089778>
- Cortese, G., Gersonde, R., Hillenbrand, C.D., Kuhn, G., 2004. Opal sedimentation shifts in the world

ocean over the last 15 Myr. *Earth Planet. Sci. Lett.* 224, 509–527.

<https://doi.org/10.1016/j.epsl.2004.05.035>

Crosta, X., Pichon, J.J., Labracherie, M., 1997. Distribution of *Chaetoceros* resting spores in modern peri-Antarctic sediments. *Mar. Micropaleontol.* 29, 283–299. [https://doi.org/10.1016/S0377-8398\(96\)00033-3](https://doi.org/10.1016/S0377-8398(96)00033-3)

Crosta, X., Romero, O., Armand, L.K., Pichon, J.J., 2005. The biogeography of major diatom taxa in Southern Ocean sediments: 2. Open ocean related species. *Palaeogeogr. Palaeoclimatol. Palaeoecol.* 223, 66–92. <https://doi.org/10.1016/j.palaeo.2005.03.028>

Dauner, A.L.L., MacCormack, W.P., Hernández, E.A., Martins, C.C., 2017. Sources and distribution of biomarkers in surficial sediments from a polar marine ecosystem (Potter Cove, King George Island, Antarctica). *Polar Biol.* 40, 2015–2025. <https://doi.org/10.1007/s00300-017-2120-5>

Demidov, A.B., Mosharov, S.A., Gagarin, V.I., Romanova, N.D., 2011. Spatial variability of the primary production and chlorophyll *a* concentration in the Drake Passage in the austral spring. *Oceanology* 51, 281–294. <https://doi.org/10.1134/S0001437011020056>

Deppeler, S.L., Davidson, A.T., 2017. Southern Ocean Phytoplankton in a Changing Climate. *Front. Mar. Sci.* 4, 1–28. <https://doi.org/10.3389/fmars.2017.00040>

DiTullio, G.R., Geesey, M.E., Jones, D.R., Daly, K., Smith, W.O., Campbell, L., 2003. Phytoplankton assemblage structure and primary productivity along 170°W in the South Pacific Ocean. *Mar. Ecol. Prog. Ser.* 255, 55–80. <https://doi.org/10.3354/meps255055>

Domack, E.W., Leventer, A., Dunbar, R., Taylor, F., Brachfeld, S., Sjunneskog, C., 2001. Chronology of the Palmer Deep site, Antarctic Peninsula: A Holocene palaeoenvironmental reference for

the circum-Antarctic. *Holocene* 11, 1–9. <https://doi.org/10.1191/095968301673881493>

Domack, E.W., Leventer, A., Root, S., Ring, J., Williams, E., Carlson, D., Hirshorn, E., Wright, W.,

Gilbert, R., Burr, G., 2003. Marine sedimentary record of natural environmental variability and recent warming in the Antarctic Peninsula. *Antarct. Penins. Clim. Var. Hist. Paleoenviron. Perspect.* 79, 205–224. <https://doi.org/10.1029/079ARS17>

Donohue, K.A., Tracey, K.L., Watts, D.R., Chidichimo, M.P., Chereskin, T.K., 2016. Mean Antarctic

Circumpolar Current transport measured in Drake Passage. *Geophys. Res. Lett.* 43, 11760–11767. <https://doi.org/10.1002/2016GL070319>

Dutkiewicz, A., Müller, R.D., O’Callaghan, S., Jónasson, H., 2015. Census of seafloor sediments in

the world’s ocean. *Geology* 43, 795–798. <https://doi.org/10.1130/G36883.1>

Esper, O., Gersonde, R., 2014a. Quaternary surface water temperature estimations: New diatom

transfer functions for the Southern Ocean. *Palaeogeogr. Palaeoclimatol. Palaeoecol.* 414, 1–19. <https://doi.org/10.1016/j.palaeo.2014.08.008>

Esper, O., Gersonde, R., 2014b. New tools for the reconstruction of Pleistocene Antarctic sea ice.

*Palaeogeogr. Palaeoclimatol. Palaeoecol.* 399, 260–283.

<https://doi.org/10.1016/j.palaeo.2014.01.019>

Esper, O., Gersonde, R., Kadagies, N., 2010. Diatom distribution in southeastern Pacific surface

sediments and their relationship to modern environmental variables. *Palaeogeogr.*

*Palaeoclimatol. Palaeoecol.* 287, 1–27. <https://doi.org/10.1016/j.palaeo.2009.12.006>

Eveleth, R., Cassar, N., Doney, S.C., Munro, D.R., Sweeney, C., 2017. Biological and physical

controls on O<sub>2</sub>/Ar, Ar and pCO<sub>2</sub> variability at the Western Antarctic Peninsula and in the

Drake Passage. *Deep. Res. Part II Top. Stud. Oceanogr.* 139, 77–88.

<https://doi.org/10.1016/j.dsr2.2016.05.002>

Ferrari, R., Provost, C., Park, Y.H., Sennéchaël, N., Garric, G., 2014. Heat fluxes across the Antarctic Circumpolar Current. *J. Geophys. Res. Ocean.* 119, 6381–6402.

<https://doi.org/10.1002/2014JC010201>

Frants, M., Gille, S.T., Hatta, M., Hiscock, W.T., Kahru, M., Measures, C.I., Greg Mitchell, B., Zhou, M., 2013. Analysis of horizontal and vertical processes contributing to natural iron supply in the mixed layer in southern Drake Passage. *Deep. Res. Part II Top. Stud. Oceanogr.* 90, 68–76.

<https://doi.org/10.1016/j.dsr2.2012.06.001>

Frölicher, T.L., Sarmiento, J.L., Paynter, D.J., Dunne, J.P., Krasting, J.P., Winton, M., 2015.

Dominance of the Southern Ocean in anthropogenic carbon and heat uptake in CMIP5 models. *J. Clim.* 28, 862–886. <https://doi.org/10.1175/JCLI-D-14-00117.1>

Gagosian, R.B., Smith, S.O., Lee, C., Farrington, J.W., Frew, N.M., 1980. Steroid transformations in recent marine sediments. *Phys. Chem. Earth* 12, 407–419. [https://doi.org/10.1016/0079-1946\(79\)90122-8](https://doi.org/10.1016/0079-1946(79)90122-8)

Geibert, W., Rutgers van der Loeff, M.M., Usbeck, R., Gersonde, R., Kuhn, G., Seeberg-Elverfeldt, J., 2005. Quantifying the opal belt in the Atlantic and southeast Pacific sector of the Southern Ocean by means of  $^{230}\text{Th}$  normalization. *Global Biogeochem. Cycles* 19, 1–13.

<https://doi.org/10.1029/2005GB002465>

Gersonde, R., Wefer, G., 1987. Sedimentation of biogenic siliceous particles in Antarctic waters from the Atlantic sector. *Mar. Micropaleontol.* 11, 311–332. [https://doi.org/10.1016/0377-8398\(87\)90004-1](https://doi.org/10.1016/0377-8398(87)90004-1)

Gersonde, R., Zielinski, U., 2000. The reconstruction of late Quaternary Antarctic sea-ice

distribution - The use of diatoms as a proxy for sea-ice. *Palaeogeogr. Palaeoclimatol.*

*Palaeoecol.* 162, 263–286. [https://doi.org/10.1016/S0031-0182\(00\)00131-0](https://doi.org/10.1016/S0031-0182(00)00131-0)

Giglio, D., Johnson, G.C., 2016. Subantarctic and Polar Fronts of the Antarctic Circumpolar Current and Southern Ocean heat and freshwater content variability: a view from Argo. *J. Phys. Oceanogr.* 46, 749–768. <https://doi.org/10.1175/JPO-D-15-0131.1>

*Oceanogr.* 46, 749–768. <https://doi.org/10.1175/JPO-D-15-0131.1>

Giordano, M., Beardall, J., Raven, J.A., 2005. CO<sub>2</sub> Concentrating Mechanisms in algae: mechanisms, environmental modulation, and evolution. *Annu. Rev. Plant Biol.* 56, 99–131.

<https://doi.org/10.1146/annurev.arplant.56.032604.144052>

Goad, L.J., Holz, G.G., Beach, D.H., 1983. Identification of (24S)-24-methylcholesta-5,22-dien-3 $\beta$ -ol as the major sterol of a marine cryptophyte and a marine prymnesiophyte. *Phytochemistry*

22, 475–476. [https://doi.org/10.1016/0031-9422\(83\)83028-3](https://doi.org/10.1016/0031-9422(83)83028-3)

Goodell, H.G., 1964. Marine geology of the Drake Passage, Scotia Sea, and South Sandwich Trench. Sedimentology Research Laboratory Contribution No. 7, Department of Geology, Florida State University, Tallahassee, 277 p.

[http://www.arf.fsu.edu/publications/documents/ELT\\_01\\_08.pdf](http://www.arf.fsu.edu/publications/documents/ELT_01_08.pdf).

Goodell, H.G., 1965. Marine geology, USNS ELTANIN Cruises 9-15. Sedimentology research laboratory contribution No. 11, Department of Geology, Florida State University,

Tallahassee, 237 p. [http://www.arf.fsu.edu/publications/documents/ELT\\_09\\_15.pdf](http://www.arf.fsu.edu/publications/documents/ELT_09_15.pdf)

Gordon, A.L., 1986. Interocean exchange of thermocline water. *J. Geophys. Res.* 91, 5037–5046.

<https://doi.org/10.1029/JC091iC04p05037>

Gordon, A.L., Nowlin, W.D., 1978. The basin waters of the Bransfield Strait. *J. Phys. Oceanogr.* 8,

258–264. <https://doi.org/10.1029/JPO8025802>

- Gradone, J.C., 2016. Surface chlorophyll variability in the Drake Passage region of the Southern Ocean. Undergraduate Honors Theses 1134. University of Colorado, Boulder, Department of Geological Science. [https://scholar.colorado.edu/honr\\_theses/1134](https://scholar.colorado.edu/honr_theses/1134)
- Harada, N., Ninnemann, U., Lange, C.B., Marchant, M.E., Sato, M., Ahagon, N., Pantoja, S., 2013. Deglacial - Holocene environmental changes at the Pacific entrance of the Strait of Magellan America. *Palaeogeogr. Palaeoclimatol. Palaeoecol.* 375, 125–135. <https://doi.org/10.1016/j.palaeo.2013.02.022>
- Harden, S.L., DeMaster, D.J., Nittrouer, C.A., 1992. Developing sediment geochronologies for high-latitude continental shelf deposits: a radiochemical approach. *Mar. Geol.* 103, 69–97. [https://doi.org/10.1016/0025-3227\(92\)90009-7](https://doi.org/10.1016/0025-3227(92)90009-7)
- Harris, P.G., Carter, J.F., Head, R.N., Harris, R.P., Eglinton, G., Maxwell, J.R., 1995. Identification of chlorophyll transformation products in zooplankton faecal pellets and marine sediment extracts by liquid chromatography/mass spectrometry atmospheric pressure chemical ionization. *Rapid Commun. Mass Spectrom.* 9, 1177–1183. <https://doi.org/10.1002/rcm.1290091218>
- Hasle, G.R., Syvertsen, E.E., 1997. Marine diatoms. In: Tomas, C.R. (Ed.), *Identify marine diatoms and dinoflagellates*. Academic Press, Inc., San Diego, pp. 5–385.
- Hass, H.C., Kuhn, G., Monien, P., Forwick, M., Sea, W., 2010. Climate fluctuations during the past two millennia as recorded in sediments from Maxwell Bay, South Shetland Islands, West Antarctica. *Geol. Soc.* 344, 243–260. <https://doi.org/10.1144/SP344.17>
- Heezen, B.C., Hollister, C., 1964. Deep-sea current evidence from abyssal sediments. *Mar. Geol.* 1, 141–174. [https://doi.org/10.1016/0025-3227\(64\)90012-X](https://doi.org/10.1016/0025-3227(64)90012-X)

- Hendry, K.R., Meredith, M.P., Ducklow, H.W., 2018. The marine system of the West Antarctic Peninsula: status and strategy for progress. *Philos. Trans. R. Soc. A* 376, 1–6.  
<https://doi.org/10.1098/rsta.2017.0179>
- Henley, S.F., Annett, A.L., Ganeshram, R.S., Carson, D.S., Weston, K., Crosta, X., Tait, A., Dougans, J., Fallick, A.E., Clarke, A., 2012. Factors influencing the stable carbon isotopic composition of suspended and sinking organic matter in the coastal Antarctic sea ice environment. *Biogeosciences* 9, 1137–1157. <https://doi.org/10.5194/bg-9-1137-2012>
- Herb, R., 1968., Recent Planktonic Foraminifera from sediments of the Drake Passage, Southern Ocean. *Eclogae Geol. Helv.* 61, 467–480.
- Herb, R., 1971. Distribution of recent benthonic foraminifera in the Drake Passage. *Biol. Antarct. Seas IV* 17, 251–300. <https://doi.org/10.1029/AR017p0251>
- Heroy, D.C., Sjunneskog, C., Anderson, J.B., 2008. Holocene climate change in the Bransfield Basin, Antarctic Peninsula: Evidence from sediment and diatom analysis. *Antarct. Sci.* 20, 69–87.  
<https://doi.org/10.1017/S0954102007000788>
- Hinke, J.T., Cossio, A.M., Goebel, M.E., Reiss, C.S., Trivelpiece, W.Z., Watters, G.M., 2017. Identifying Risk: concurrent overlap of the antarctic krill fishery with krill-dependent predators in the Scotia Sea. *PLoS One* 12, 1–24.  
<https://doi.org/10.1371/journal.pone.0170132>
- Holm-Hansen, O., Mitchell, B.G., 1991. Spatial and temporal distribution of phytoplankton and primary production in the western Bransfield Strait region. *Deep. Res.* 38, 961–980.
- Honjo, S., Francois, R., Manganini, S., Dymond, J., Collier, R., 2000. Particle fluxes to the interior of the Southern Ocean in the western Pacific sector along 170°W. *Deep. Res. Part II Top. Stud.*

Oceanogr. 47, 3521–3548. [https://doi.org/10.1016/S0967-0645\(00\)00077-1](https://doi.org/10.1016/S0967-0645(00)00077-1)

Honjo, S., 2004. Particle export and the biological pump in the Southern Ocean. *Antarct. Sci.* 16, 501–516. <https://doi.org/10.1017/S0954102004002287>

Ichii, T., Katayama, K., Obitsu, N., Ishii, H., Naganobu, M., 1998. Occurrence of Antarctic krill (*Euphausia superba*) concentrations in the vicinity of the South Shetland Islands: relationship to environmental parameters. *Deep. Res. Part I Oceanogr. Res. Pap.* 45, 1235–1262.

Isla, E., Masqué, P., Palanques, A., Guillén, J., Puig, P., Sanchez-Cabeza, J.A., 2004. Sedimentation of biogenic constituents during the last century in western Bransfield and Gerlache Straits, Antarctica: A relation to currents, primary production, and sea floor relief. *Mar. Geol.* 209, 265–277. <https://doi.org/10.1016/j.margeo.2004.06.003>

Isla, E., 2016. Organic carbon and biogenic silica in marine sediments in the vicinities of the Antarctic Peninsula: spatial patterns across a climatic gradient. *Polar Biol.* 39, 819–828. <https://doi.org/10.1007/s00300-015-1833-6>

Jeffrey, S.W., Humphrey, G.F., 1975. New spectrophotometric equations for determining chlorophylls a, b, c<sub>1</sub> and c<sub>2</sub> in higher plants, algae and natural phytoplankton. *Biochem. und Physiol. der Pflanz.* 167, 191–194. [https://doi.org/10.1016/S0015-3796\(17\)30778-3](https://doi.org/10.1016/S0015-3796(17)30778-3)

Kim, Y.S., Orsi, A.H., 2014. On the variability of Antarctic Circumpolar Current fronts inferred from 1992–2011 Altimetry. *J. Phys. Oceanogr.* 44, 3054–3071. <https://doi.org/10.1175/JPO-D-13-0217.1>

Klöser, H., Quartino, M.L., Wiencke, C., 1996. Distribution of macroalgae and macroalgal communities in gradients of physical conditions in Potter Cove, King George Island, Antarctica. *Hydrobiologia* 333, 1–17. <https://doi.org/10.1007/BF00020959>

- Klunder, M.B., Laan, P., De Baar, H.J.W., Middag, R., Neven, I., Van Ooijen, J., 2014. Dissolved Fe across the Weddell Sea and Drake Passage: Impact of DFe on nutrient uptake. *Biogeosciences* 11, 651–669. <https://doi.org/10.5194/bg-11-651-2014>
- Kopczynska, E.E., Dehairs, F., Elskens, M., Wright, S., 2001. Phytoplankton and microzooplankton variability between the Subtropical and Polar Fronts south of Australia: Thriving under regenerative and new production in late summer. *J. Geophys. Res.* 106, 31597–31609. <https://doi.org/10.1029/2000JC000278>
- Kuhn, G., 2014. Don't forget the salty soup : Calculations for bulk marine geochemistry and radionuclide geochronology. *Mineral. Mag.* 77(5), 1519. <https://www.researchgate.net/publication/257941084>
- Ladant, J.B., Donnadieu, Y., Bopp, L., Lear, C.H., Wilson, P.A., 2018. Meridional contrasts in productivity changes driven by the opening of Drake Passage. *Paleoceanogr. Paleoclimatology* 33, 302–317. <https://doi.org/10.1002/2017PA003211>
- Lamy, F., 2016. The Expedition PS97 of the Research Vessel POLARSTERN to the Drake Passage in 2016 , *Berichte zur Polar- und Meeresforschung = Reports on polar and marine research*, Bremerhaven, Alfred Wegener Institute for Polar and Marine Research, 701, 571 pp. [https://doi.org/10.2312/BzPM\\_0702\\_2016](https://doi.org/10.2312/BzPM_0702_2016)
- Lamy, F., Arz, H.W., Kilian, R., Lange, C.B., Lembke-Jene, L., Wengler, M., Kaiser, J., Baeza-Urrea, O., Hall, I.R., Harada, N., Tiedemann, R., 2015. Glacial reduction and millennial-scale variations in Drake Passage throughflow. *Proc. Natl. Acad. Sci.* 112, 13496–13501. <https://doi.org/10.1073/pnas.1509203112>
- Lange, C.B., Rebolledo, L., Schulz, H., Müller, J., Arz, H., Lamy, F., PS97 Shipboard Party, 2016.

Composition of surface sediments across the Drake Passage related to ocean productivity, terrigenous input, currents, and ice proximity. International Conference on Paleooceanography, August 29<sup>th</sup> to September 2<sup>nd</sup>, 2016. Utrecht, The Netherlands. Poster #P-180.

Learman, D.R., Henson, M.W., Thrash, J.C., Temperton, B., Brannock, P.M., Santos, S.R., Mahon, A.R., Halanych, K.M., 2016. Biogeochemical and microbial variation across 5500 km of Antarctic surface sediment implicates organic matter as a driver of benthic community structure. *Front. Microbiol.* 7, 1–11. <https://doi.org/10.3389/fmicb.2016.00284>

Leavitt, P.R., Hudgson, D., 2001. Sedimentary Pigments, in: Smol, J.P., Birks, H.J.B., Last, W.M. (Eds.), *Tracking Environmental Change using Lake Sediments. Volume 3: Terrestrial, Algal, and Siliceous Indicators*. Kluwer Academic Publishers, Dordrecht, The Netherlands, pp. 295–325.

Leavitt, P.R., 1993. A review of factors that regulate carotenoid and chlorophyll deposition and fossil pigment abundance. *J. Paleolimnol.* 9, 109–127. <https://doi.org/10.1007/BF00677513>

Lee, C., Wakeham, S.G., I. Hedges, J., 2000. Composition and flux of particulate amino acids and chloropigments in equatorial Pacific seawater and sediments, *Deep. Res. Part I Oceanogr. Res. Pap.* 47, 1535–1568. [https://doi.org/10.1016/S0967-0637\(99\)00116-8](https://doi.org/10.1016/S0967-0637(99)00116-8)

Leventer, A., 1991. Sediment trap diatom assemblages from the northern Antarctic Peninsula region. *Deep. Res. Part I Oceanogr. Res. Pap.* 38, 1127–1143. [https://doi.org/10.1016/0198-0149\(91\)90099-2](https://doi.org/10.1016/0198-0149(91)90099-2)

Leventer, A., 1992. Modern distribution of diatoms in sediments from the George V Coast, Antarctica. *Mar. Micropaleontol.* 19, 315–332. [https://doi.org/10.1016/0377-8398\(92\)00037-8](https://doi.org/10.1016/0377-8398(92)00037-8)

- Majewski, W., Wellner, J.S., Szczuciński, W., Anderson, J.B., 2012. Holocene oceanographic and glacial changes recorded in Maxwell Bay, West Antarctica. *Mar. Geol.* 326–328, 67–79.  
<https://doi.org/10.1016/j.margeo.2012.08.009>
- Malainey, M., Álvarez, M., Briz i Godino, I., Zurro, D., Verdún i Castelló, E., Figol, T., 2015. The use of shells as tools by hunters-gatherers in the Beagle Channel (Tierra del Fuego, South America): an ethnoarchaeological experiment. *Archaeol. Anthropol. Sci.* 7, 187–200.  
<https://doi.org/10.1007/s12520-014-0188-1>
- Mantoura, R.F.C., Llewellyn, C.A., 1983. The rapid determination of algal chlorophyll and carotenoid pigments and their breakdown products in natural waters by reverse-phase high-performance liquid chromatography. *Anal. Chim. Acta* 151, 297–314.  
[https://doi.org/10.1016/S0003-2670\(00\)80092-6](https://doi.org/10.1016/S0003-2670(00)80092-6)
- Marinov, I., Gnanadesikan, A., Toggweiler, J.R., Sarmiento, J.L., 2006. The Southern Ocean biogeochemical divide. *Nature* 441, 964–967. <https://doi.org/10.1038/nature04883>
- Marrari, M., Daly, K.L., Hu, C., 2008. Spatial and temporal variability of SeaWiFS chlorophyll *a* distributions west of the Antarctic Peninsula: Implications for krill production. *Deep. Res. Part II Top. Stud. Oceanogr.* 55, 377–392. <https://doi.org/10.1016/j.dsr2.2007.11.011>
- Marshall, J., Speer, K., 2012. Closure of the meridional overturning circulation through Southern Ocean upwelling. *Nat. Geosci.* 5, 171–180. <https://doi.org/10.1038/ngeo1391>
- Martin, J.H., Gordon, R.M., Fitzwater, S.E., 1990. Iron in Antarctic waters. *Nature* 345, 156–158.  
<https://doi.org/10.1038/345156a0>
- Masqué, P., Isla, E., Sanchez-Cabeza, J.A., Palanques, A., Bruach, J.M., Puig, P., Guillén, J., 2002. Sediment accumulation rates and carbon fluxes to bottom sediments at the Western

Bransfield Strait (Antarctica). *Deep Sea Res. Part II Top. Stud. Oceanogr.* 49, 921–933.

[https://doi.org/http://dx.doi.org/10.1016/S0967-0645\(01\)00131-X](https://doi.org/http://dx.doi.org/10.1016/S0967-0645(01)00131-X)

Meredith, M.P., Woodworth, P.L., Chereskin, T.K., Marshall, D.P., Allison, L.C., Bigg, G.R., Donohue, K., Heywood, K.J., Hughes, C.W., Hibbert, A., Hogg, A.M., Johnson, H.L., Jullion, L., King, B.A., Leach, H., Lenn, Y.D., Morales Maqueda, M.A., Munday, D.R., Naveira Garabato, A.C., Provost, C., Sallée, J. B., Sprintall, J., 2011. Sustained monitoring of the Southern Ocean at Drake Passage: past achievements and future priorities. *Rev. Geophys.* 49, 1–36.

<https://doi.org/10.1029/2010RG000348>

Meredith, M.P., Falk, U., Bers, A.V., Mackensen, A., Schloss, I.R., Barlett, E.R., Jerosch, K., Silva, A., Abele, D., 2018. Anatomy of a glacial meltwater discharge event in an Antarctic cove. *Philos. Trans. R. Soc. A* 376, 20170163. <https://doi.org/10.1098/rsta.2017.0163>

Milliken, K.T., Anderson, J.B., Wellner, J.S., Bohaty, S.M., Manley, P.L., 2009. High-resolution Holocene climate record from Maxwell Bay, South Shetland Islands, Antarctica. *Bull. Geol. Soc. Am.* 121, 1711–1725. <https://doi.org/10.1130/B26478.1>

Mincks, S.L., Smith, C.R., Jeffreys, R.M., Sumida, P.Y.G., 2008. Trophic structure on the West Antarctic Peninsula shelf: Detritivory and benthic inertia revealed by  $\delta^{13}\text{C}$  and  $\delta^{15}\text{N}$  analysis. *Deep. Res. Part II Top. Stud. Oceanogr.* 55, 2502–2514.

<https://doi.org/10.1016/j.dsr2.2008.06.009>

Moffat, C., Meredith, M., 2018. Shelf-ocean exchange and hydrography west of the Antarctic Peninsula: a review. *Philos. Trans. R. Soc. A* 376, 20170164.

<https://doi.org/10.1098/rsta.2017.0164>

Moore, J.K., Abbott, M.R., 2000. Phytoplankton chlorophyll distributions and primary production

in the Southern Ocean. *J. Geophys. Res.* 105, 28709–28722.

<https://doi.org/10.1029/2007JG000640/abstract>

Morrison, A.K., Frölicher, T.L., Sarmiento, J.L., 2015. Upwelling in the Southern Ocean. *Am. Inst.*

*Phys.* 68, 1–27. <https://doi.org/10.1063/PT.3.2654> View

Mortlock, R.A., Froelich, P.N., 1989. A simple method for the rapid determination of biogenic opal

in pelagic marine sediments. *Deep Res.* 36, 1415–1426. <https://doi.org/10.1016/0198->

0149(89)90092-7

Müller, P.J., Schneider, R., 1993. An automated leaching method for the determination of opal in

sediments and particulate matter. *Deep. Res. Part I Oceanogr. Res. Pap.* 40, 425–444.

[https://doi.org/10.1016/0967-0637\(93\)90140-X](https://doi.org/10.1016/0967-0637(93)90140-X)

Munro, D.R., Lovenduski, N.S., Stephens, B.B., Newberger, T., Arrigo, K.R., Takahashi, T., Quay,

P.D., Sprintall, J., Freeman, N.M., Sweeney, C., 2015. Estimates of net community production

in the Southern Ocean determined from time series observations (2002 – 2011) of nutrients,

dissolved inorganic carbon, and surface ocean pCO<sub>2</sub> in Drake Passage. *Deep. Res. Part II Top.*

*Stud. Oceanogr.* 114, 49–63. <https://doi.org/10.1016/j.dsr2.2014.12.014>

Munro, D.R., Lovenduski, N.S., Takahashi, T., Stephens, B.B., Newberger, T., Sweeney, C., 2015.

Recent evidence for a strengthening CO<sub>2</sub> sink in the Southern Ocean from carbonate system

measurements in the Drake Passage (2002 – 2015). *Geophys. Res. Lett.* 42, 7623–7630.

<https://doi.org/10.1002/2015GL065194>

Nelson, D.M., Anderson, R.F., Barber, R.T., Brzezinski, M.A., Buesseler, K.O., Chase, Z., Collier, R.W.,

Dickson, M.L., François, R., Hiscock, M.R., Honjo, S., Marra, J., Martin, W.R., Sambrotto, R.N.,

Sayles, F.L., Sigmon, D.E., 2002. Vertical budgets for organic carbon and biogenic silica in the

Pacific sector of the Southern Ocean, 1996-1998. *Deep. Res. Part II Top. Stud. Oceanogr.* 49, 1645–1674. [https://doi.org/10.1016/S0967-0645\(02\)00005-X](https://doi.org/10.1016/S0967-0645(02)00005-X)

Nelson, M.M., Mooney, B.D., Nichols, P.D., Phleger, C.F., 2001. Lipids of Antarctic Ocean amphipods: Food chain interactions and the occurrence of novel biomarkers. *Mar. Chem.* 73, 53–64. [https://doi.org/10.1016/S0304-4203\(00\)00072-4](https://doi.org/10.1016/S0304-4203(00)00072-4)

Nghiem, S. V., Rigor, I.G., Clemente-Colón, P., Neumann, G., Li, P.P., 2016. Geophysical constraints on the Antarctic sea ice cover. *Remote Sens. Environ.* 181, 281–292. <https://doi.org/10.1016/j.rse.2016.04.005>

Orsi, A.H., Whitworth, T., Nowlin, W.D., 1995. On the meridional extent and fronts of the Antarctic Circumpolar Current. *Deep. Res. Part I Oceanogr. Res. Pap.* 42, 641–673. [https://doi.org/10.1016/0967-0637\(95\)00021-W](https://doi.org/10.1016/0967-0637(95)00021-W)

Palanques, A., Isla, E., Puig, P., Sanchez-Cabeza, J.A., Masqué, P., 2002. Annual evolution of downward particle fluxes in the Western Bransfield Strait (Antarctica) during the FRUELA project. *Deep. Res. Part II Top. Stud. Oceanogr.* 49, 903–920. [https://doi.org/10.1016/S0967-0645\(01\)00130-8](https://doi.org/10.1016/S0967-0645(01)00130-8)

Paparazzo, F.E., Alder, V.A., Schloss, I.R., Bianchi, A., Esteves, J.L., 2016. Spatial and temporal trends in the distribution of macronutrients in surface waters of the Drake Passage. *Ecol. Austral* 26, 27–39. [http://www.scielo.org.ar/scielo.php?script=sci\\_arttext&pid=S1667-782X2016000100004&lng=es&tlng=en](http://www.scielo.org.ar/scielo.php?script=sci_arttext&pid=S1667-782X2016000100004&lng=es&tlng=en)

Pereira, C.M.P., Nunes, C.F.P., Zambotti-Villela, L., Streit, N.M., Dias, D., Pinto, E., Gomes, C.B., Colepicolo, P., 2017. Extraction of sterols in brown macroalgae from Antarctica and their identification by liquid chromatography coupled with tandem mass spectrometry. *J. Appl.*

Phycol. 29, 751–757. <https://doi.org/10.1007/s10811-016-0905-5>

Phleger, C.F., Nelson, M.M., Mooney, B., Nichols, P.D., 2000. Lipids of Antarctic salps and their commensal hyperiid amphipods. *Polar Biol.* 23, 329–337.

<https://doi.org/10.1007/s003000050452>

Phleger, C.F., Nichols, P.D., Virtue, P., 1998. Lipids and trophodynamics of Antarctic zooplankton. *Comp. Biochem. Physiol.* 120, 311–323. [https://doi.org/10.1016/S0305-0491\(98\)10020-2](https://doi.org/10.1016/S0305-0491(98)10020-2)

Pichon, J.J., Bareille, G., Labracherie, M., Labeyrie, L.D., Baudrimont, A., Turon, J.L., 1992.

Quantification of the biogenic silica dissolution in Southern Ocean sediments. *Quat. Res.* 37, 361–378. [https://doi.org/10.1016/0033-5894\(92\)90073-R](https://doi.org/10.1016/0033-5894(92)90073-R)

Pollard, R., Tréguer, P., Read, J., 2006. Quantifying nutrient supply to the Southern Ocean. *J.*

*Geophys. Res. Ocean.* 111, 1–9. <https://doi.org/10.1029/2005JC003076>

Pondaven, P., Ragueneau, O., Tréguer, P., Hauvespre, A., Dezileau, L., Reyss, J.L., 2000. Resolving the “opal paradox” in the Southern Ocean. *Nature* 405, 168–172.

<https://doi.org/10.1038/35012046>

Popp, B.N., Trull, T., Kenig, F., Wakeham, S.G., Rust, T.M., Tilbrook, B., Griffiths, B., Wright, S.W., Marchant, H.J., Bidigare, R.R., Laws, E.A., 1999. Controls on the carbon isotopic composition of Southern Ocean phytoplankton. *Glob. Biogeochem. Cycles* 13, 827–843.

<https://doi.org/10.1029/1999GB900041>

Provost, C., Renault, A., Barré, N., Sennéchaël, N., Garçon, V., Sudre, J., Huhn, O., 2011. Two repeat crossings of Drake Passage in austral summer 2006: Short-term variations and evidence for considerable ventilation of intermediate and deep waters. *Deep. Res. Part II Top. Stud.*

*Oceanogr.* 58, 2555–2571. <https://doi.org/10.1016/j.dsr2.2011.06.009>

- Ragueneau, O., Dittert, N., Pondaven, P., Tréguer, P., Corrin, L., 2002. Si/C decoupling in the world ocean: Is the Southern Ocean different? *Deep. Res. Part II Top. Stud. Oceanogr.* 49, 3127–3154. [https://doi.org/10.1016/S0967-0645\(02\)00075-9](https://doi.org/10.1016/S0967-0645(02)00075-9)
- Rampen, S.W., Abbas, B.A., Schouten, S., Damsté, J.S.S., 2010. A comprehensive study of sterols in marine diatoms (Bacillariophyta): Implications for their use as tracers for diatom productivity. *Limnol. Oceanogr.* 55, 91–105. <https://doi.org/10.4319/lo.2010.55.1.0091>
- R Core Team., 2017. R: A language and environment for statistical computing. R Foundation for Statistical Computing, Vienna, Austria. <https://www.R-project.org/>
- Rigual-Hernández, A.S., Trull, T.W., Bray, S.G., Cortina, A., Armand, L.K., 2015. Latitudinal and temporal distributions of diatom populations in the pelagic waters of the Subantarctic and Polar Frontal zones of the Southern Ocean and their role in the biological pump. *Biogeosciences* 12, 5309–5337. <https://doi.org/10.5194/bg-12-5309-2015>
- Rintoul, S.R., 2009. Antarctic Circumpolar Current, in: Steele, J.H., Turekian, K.K., Thorpe, S.A. (Eds), *Encyclopedia of Ocean Sciences. Antarctic Climate and Ecosystems Cooperative Research Centre, Australia, Tasmania*, pp. 178–190. <https://doi.org/10.1016/B978-012374473-9.00603-2>
- Rintoul, S.R., 2018. The global influence of localized dynamics in the Southern Ocean. *Nature* 558, 209–218. <https://doi.org/10.1038/s41586-018-0182-3>
- Romero, O.E., Armand, L.K., Crosta, X., Pichon, J.J., 2005. The biogeography of major diatom taxa in Southern Ocean surface sediments: 3. Tropical/Subtropical species. *Palaeogeogr. Palaeoclimatol. Palaeoecol.* 223, 49–65. <https://doi.org/10.1016/j.palaeo.2005.03.027>
- Rontani, J.F., Charrière, B., Sempéré, R., Doxaran, D., Vaultier, F., Vonk, J.E., Volkman, J.K., 2014.

Degradation of sterols and terrigenous organic matter in waters of the Mackenzie Shelf,  
Canadian Arctic. *Org. Geochem.* 75, 61–73.

<https://doi.org/10.1016/j.orggeochem.2014.06.002>

Rozema, P.D., Kulk, G., Veldhuis, M.P., Buma, A.G.J., Meredith, M.P., van de Poll, W.H., 2017.

Assessing drivers of coastal primary production in northern Marguerite Bay, Antarctica.

*Front. Mar. Sci.* 4, 1–20. <https://doi.org/10.3389/fmars.2017.00184>

Sangrà, P., Gordo, C., Hernández-Arencibia, M., Marrero-Díaz, A., Rodríguez-Santana, A., Stegner,

A., Martínez-Marrero, A., Pelegrí, J.L., Pichon, T., 2011. The Bransfield current system. *Deep.*

*Res. Part I Oceanogr. Res. Pap.* 58, 390–402. <https://doi.org/10.1016/j.dsr.2011.01.011>

Sangrà, P., Stegner, A., Hernández-Arencibia, M., Marrero-Díaz, A., Salinas, C., Aguiar-González, B.,

Henríquez-Pastene, C., Mouriño-Carballido, B., 2017. The Bransfield Gravity Current. *Deep.*

*Res. Part I Oceanogr. Res. Pap.* 119, 1–15. <https://doi.org/10.1016/j.dsr.2016.11.003>

Sañé, E., Isla, E., Grémare, A., Gutt, J., Vétion, G., DeMaster, D.J., 2011. Pigments in sediments

beneath recently collapsed ice shelves: The case of Larsen A and B shelves, Antarctic

Peninsula. *J. Sea Res.* 65, 94–102. <https://doi.org/10.1016/j.seares.2010.07.005>

Sarmiento, J.L., Gruber, N., Brzezinski, M.A., Dunne, J.P., 2004. High-latitude controls of

thermocline nutrients and low latitude biological productivity. *Nature* 479, 556–556.

<https://doi.org/10.1038/nature10605>

Sauer, P.E., Eglinton, T.I., Hayes, J.M., Schimmelmann, A., Sessions, A.L., 2001. Compound-specific

D/H ratios of lipid biomarkers from sediments as a proxy for environmental and climatic

conditions. *Geochim. Cosmochim. Acta* 65, 213–222. <https://doi.org/10.1016/S0016->

7037(00)00520-2

- Schrader, H.J., Gersonde, R., 1978. Diatoms and silicofagellates. Micro-paleontological counting methods and techniques: an exercise on an eight metres section of the Lower Pliocene of Capo Rosello, Sicily. *Utrecht Micropaleontology Bulletin* 17, 129–176.
- Shannon, C., 1948., A mathematical theory of communication. *The Bell System Technical Journal* 27, 379–423. <https://doi.org/10.1002/j.1538-7305.1948.tb01338.x>
- Smith, C.R., Mincks, S., DeMaster, D.J., 2008. The FOODBANCS project: Introduction and sinking fluxes of organic carbon, chlorophyll-*a* and phytodetritus on the western Antarctic Peninsula continental shelf. *Deep. Res. Part II Top. Stud. Oceanogr.* 55, 2404–2414.  
<https://doi.org/10.1016/j.dsr2.2008.06.001>
- Sokolov, S., Rintoul, S.R., 2007. On the relationship between fronts of the Antarctic Circumpolar Current and surface chlorophyll concentrations in the Southern Ocean. *J. Geophys. Res. Ocean.* 112, 1–17. <https://doi.org/10.1029/2006JC004072>
- Sokolov, S., Rintoul, S.R., 2009. Circumpolar structure and distribution of the Antarctic Circumpolar Current fronts: 1. Mean circumpolar paths. *J. Geophys. Res. Ocean.* 114, 1–19.  
<https://doi.org/10.1029/2008JC005108>
- Sprintall, J., 2003. Seasonal to interannual upper-ocean variability in the Drake Passage. *J. Mar. Res.* 61, 27–57. <https://doi.org/10.1357/002224003321586408>
- Sprintall, J., Chereskin, T., Sweeney, C., 2012. High-resolution underway upper ocean and surface atmospheric observations in Drake Passage: synergistic measurements for climate science. *Oceanography* 25, 70–81. <https://doi.org/10.5670/oceanog.2012.77>
- Sun, M.Y., Aller, R.C., Lee, C., 1991. Early diagenesis of chlorophyll *a* in Long Island Sound sediments: A measure of carbon flux and particle reworking. *Journal of Marine Research* 49,

379–401. <https://doi.org/10.1357/002224091784995927>

Sun, M.Y., Aller, R.C., Lee, C., 1994. Spatial and temporal distributions of sedimentary chloropigments as indicators of benthic processes in Long-Island Sound. *J. Mar. Res.* 52, 149–176. <https://doi.org/10.1357/0022240943076768>

Sun, M.Y., Lee, C., Aller, R.C., 1993. Laboratory studies of oxic and anoxic degradation of chlorophyll-*a* in Long Island Sound sediments. *Geochim. Cosmochim. Acta* 57, 147–157. [https://doi.org/10.1016/0016-7037\(93\)90475-C](https://doi.org/10.1016/0016-7037(93)90475-C)

Świło, M., Majewski, W., Minzoni, R.T., Anderson, J.B., 2016. Diatom assemblages from coastal settings of West Antarctica. *Mar. Micropaleontol.* 125, 95–109. <https://doi.org/10.1016/j.marmicro.2016.04.001>

Szymczak-Zyła, M., Kowalewska, G., Louda, J.W., 2011. Chlorophyll-*a* and derivatives in recent sediments as indicators of productivity and depositional conditions. *Mar. Chem.* 125, 39–48. <https://doi.org/10.1016/j.marchem.2011.02.002>

Taylor, F., Whitehead, J., Domack, E., 2001. Holocene paleoclimate change in the Antarctic Peninsula: Evidence from the diatom, sedimentary and geochemical record. *Mar. Micropaleontol.* 41, 25–43. [https://doi.org/10.1016/S0377-8398\(00\)00049-9](https://doi.org/10.1016/S0377-8398(00)00049-9)

Thompson, G.A., Dinofrio, E.O., Alder, V.A., 2012. Interannual fluctuations in copepod abundance and contribution of small forms in the Drake Passage during austral summer. *Helgol. Mar. Res.* 66, 127–138. <https://doi.org/10.1007/s10152-011-0253-4>

Toggweiler, J.R., Bjornsson, H., 2000. Drake Passage and palaeoclimate. *J. Quat. Sci.* 15, 319–328. [https://doi.org/10.1002/1099-1417\(200005\)](https://doi.org/10.1002/1099-1417(200005))

Tréguer, P.J., 2014. The Southern Ocean silica cycle. *Comptes Rendus - Geosci.* 346, 279–286.

<https://doi.org/10.1016/j.crte.2014.07.003>

Tréguer, P.J., De La Rocha, C.L., 2013. The world ocean silica cycle. *Ann. Rev. Mar. Sci.* 5, 477–501.

<https://doi.org/10.1146/annurev-marine-121211-172346>

Trull, T.W., Rintoul, S.R., Hadfield, M., Abraham, E.R., 2001. Circulation and seasonal evolution of polar waters south of Australia: implications for iron fertilization of the Southern Ocean.

*Deep. Res. Part II Top. Stud. Oceanogr.* 48, 2439–2466. [https://doi.org/10.1016/S0967-0645\(01\)00003-0](https://doi.org/10.1016/S0967-0645(01)00003-0)

Veit-Köhler, G., Durst, S., Schuckebrook, J., Hauquier, F., Durán Suja, L., Dorschel, B., Vanreusel, A., Martínez Arbizu, P., 2018. Oceanographic and topographic conditions structure benthic meiofauna communities in the Weddell Sea, Bransfield Strait and Drake Passage (Antarctic).

*Prog. Oceanogr.* 162, 240–256. <https://doi.org/10.1016/j.pocean.2018.03.005>

Venables, H., Moore, C.M., 2010. Phytoplankton and light limitation in the Southern Ocean: Learning from high-nutrient, high-chlorophyll areas. *J. Geophys. Res.* 115, 1–12.

<https://doi.org/10.1029/2009jc005361>

Venkatesan, M.I., Kaplan, I.R., 1987. The lipid geochemistry of Antarctic marine sediments:

Bransfield Strait. *Mar. Chem.* 21, 347–375. [https://doi.org/10.1016/0304-4203\(87\)90056-9](https://doi.org/10.1016/0304-4203(87)90056-9)

Vernet, M., Lorenzen, C.J., 1987. The relative abundance of phaeophorbide *a* and pheophytin *a* in temperature marine waters. *Limnol. Oceanogr.* 32, 352–358.

<https://doi.org/10.4319/lo.1987.32.2.0352>

Vernet, M., Martinson, D., Iannuzzi, R., Stammerjohn, S., Kozłowski, W., Sines, K., Smith, R., Garibotti, I., 2008. Primary production within the sea-ice zone west of the Antarctic

Peninsula: I-Sea ice, summer mixed layer, and irradiance. *Deep. Res. Part II Top. Stud.*

Oceanogr. 55, 2068–2085. <https://doi.org/10.1016/j.dsr2.2008.05.021>

Villanueva, J., Hastings, D.W., 2000. A century-scale record of the preservation of chlorophyll and its transformation products in anoxic sediments. *Geochim. Cosmochim. Acta* 64, 2281–2294. [https://doi.org/10.1016/S0016-7037\(99\)00428-7](https://doi.org/10.1016/S0016-7037(99)00428-7)

Villinski, J.C., Hayes, J.M., Brassell, S.C., Riggert, V.L., Dunbar, R.B., 2008. Sedimentary sterols as biogeochemical indicators in the Southern Ocean. *Org. Geochem.* 39, 567–588. <https://doi.org/10.1016/j.orggeochem.2008.01.009>

Volkman, J.K., 1986. A review of sterol markers for marine and terrigenous organic matter. *Org. Geochem.* 9, 83–99. [https://doi.org/10.1016/0146-6380\(86\)90089-6](https://doi.org/10.1016/0146-6380(86)90089-6)

Volkman, J.K., 2003. Sterols in microorganisms. *Appl. Microbiol. Biotechnol.* 60, 495–506. <https://doi.org/10.1007/s00253-002-1172-8>

Volkman, J.K., Barrett, S.M., Dunstan, G.A., Jeffrey, S.W., 1993. Geochemical significance of the occurrence of dinosterol and other 4-methyl sterols in a marine diatom. *Org. Geochem.* 20, 7–15. [https://doi.org/10.1016/0146-6380\(93\)90076-N](https://doi.org/10.1016/0146-6380(93)90076-N)

Wadley, M.R., Jickells, T.D., Heywood, K.J., 2014. The role of iron sources and transport for Southern Ocean productivity. *Deep. Res. Part I Oceanogr. Res. Pap.* 87, 82–94. <https://doi.org/10.1016/j.dsr.2014.02.003>

Wakeham, S.G., Lee, C., Hedges, J.I., Hernes, P.J., Peterson, M.L., 1997. Molecular indicators of diagenetic status in marine organic matter. *Geochim. Cosmochim. Acta* 61, 5363–5369.

Wisnieski, E., Bicego, M.C., Montone, R.C., Figueira, R.C.L., Ceschim, L.M.M., Mahiques, M.M., Martins, C.C., 2014. Characterization of sources and temporal variation in the organic matter input indicated by n-alkanols and sterols in sediment cores from Admiralty Bay, King George

Island, Antarctica. *Polar Biol.* 37, 483–496. <https://doi.org/10.1007/s00300-014-1445-6>

Yoon, H. Il, Yoo, K.C., Bak, Y.S., Lee, Y. Il, Lee, J. Il, 2009. Core-based reconstruction of paleoenvironmental conditions in the southern Drake Passage (West Antarctica) over the last 150 ka. *Geo-Marine Lett.* 29, 309–320. <https://doi.org/10.1007/s00367-009-0144-8>

Zhou, M., Niiler, P.P., Zhu, Y., Dorland, R.D., 2006. The western boundary current in the Bransfield Strait, Antarctica. *Deep. Res. Part I Oceanogr. Res. Pap.* 53, 1244–1252. <https://doi.org/10.1016/j.dsr.2006.04.003>

Zielinski, U., Gersonde, R., 1997. Diatom distribution in Southern Ocean surface sediments (Atlantic sector): Implications for paleoenvironmental reconstructions. *Palaeogeogr. Palaeoclimatol. Palaeoecol.* 129, 213–250. [https://doi.org/10.1016/S0031-0182\(96\)00130-7](https://doi.org/10.1016/S0031-0182(96)00130-7)

**Table Captions**

Table 1. Sterols recorded in surface sediments of the study area, with their possible sources.

Table 2. Diatoms recorded in surface sediments of the study area. Taxon name, abbreviation code and range of relative abundance (min/max). See also Fig. 7.

Table 3. Correlation matrix of the 12 proxies included in the PCA (Fig. 8). The grey shadings highlight significant correlations (p-value < 0.05).

## Figure Captions

Figure 1. a) Location of PS97 surface sediment sampling sites (yellow dots) from the Chilean/Argentinian continental margin to the Antarctic Peninsula. Detailed locations are provided in Table S1. Background is the bathymetry of Drake Passage area obtained from ETOPO 1 database (Amante and Eakins, 2009). ACC= Antarctic Circumpolar Current, CHC= Cape Horn Current, SSI= South Shetland Islands. SAF=Subantarctic Front; PF=Polar Front, SACCF= Southern Antarctic Circumpolar Current Front, after Orsi et al. (1995). SAZ=Subantarctic Zone, PFZ + POOZ= Polar Front Zone + Permanently Open Ocean Zone, TZ=Transitional Zone encompassing three sites on the Antarctic continental margin, and sSIZ= seasonal Sea-Ice Zone. Maximum sea-ice extent in winter (mean 1979-2009 from the Australian Antarctic Data Centre, <https://www1.data.antarctica.gov.au/>). b) Detail of sampling sites in the Antarctic Peninsula (AP) area. Overview of the circulation on the western of AP shelf according to Moffat and Meredith (2018). c) 2015 summer and winter mean sea surface temperature (°C) obtained from Woods Hole Oceanographic Institution (WHOI) OAFlux Project (<http://oaflux.whoi.edu/index.html>).

Figure 2. Spatial distribution of bulk sediment composition in surface sediments of the study area expressed as percentages of (a) siliciclastic content (wt.%), (b) carbonates ( $\text{CaCO}_3$ , wt.%), (c) biogenic opal (wt.%), and total organic carbon (TOC, wt.%). Data are presented in Table S1. Background is the bathymetry of the Drake Passage area obtained from the ETOPO 1 database (Amante and Eakins, 2009). Fronts SAF, PF and SACCF, after Orsi et al. (1995), as in Fig. 1.

Figure 3. Spatial distribution of C/N molar ratio (a),  $\delta^{13}\text{C}_{\text{org}}$  (‰) (b), and  $\delta^{15}\text{N}$  (‰) (c) in surface sediments of the study area. Fronts SAF, PF and SACCF, after Orsi et al. (1995), as in Fig. 1. Data are presented in Table S1.

Figure 4. Spatial variability of organic geochemistry parameters in surface sediments of the study area expressed as: (a) percent total organic carbon (TOC wt.%) and concentrations of (b) total pigments, (c) total chlorophyll, (d) phaeopigments, and (e) total sterols. All concentrations are standardized by TOC ( $\mu\text{g/g}$  TOC). Stations are arranged from N to S with respect to fronts (SAF, PF and SACCF, after Orsi et al., 1995). DP= Drake Passage, SSI= South Shetland Islands, BS= Bransfield Strait. Data are presented in Table S1.

Figure 5. Spatial variability of sterols in the study area. Relative abundance of sterols (upper panel) and diversity index (Shannon-Wiener; lower panel). Stations are arranged from N to S with respect to fronts (SAF, PF and SACCF, after Orsi et al., 1995). Abbreviations SSI and BS as in Fig. 4. Data are presented in Table S2. See also Table 1 in main text.

Figure 6. Diatom concentration ( $10^6$  valves/g dry sediment) and preservation in selected surface sediment samples of the study area (preservation range: g–m= good–moderate, m= moderate, m–p= moderate–poor, after Esper et al., 2010). Background is the bathymetry of the Drake Passage area (ODV). Fronts SAF, PF and SACCF, after Orsi et al. (1995). Data are presented in Table S3.

Figure 7. Principal Component Analysis (PCA) biplot showing the relationship between 42 diatom species in 24 surface sediments (Tables S4 and S5) in response to changing environmental gradients. PC1 represents 44.9% of the variance and PC2 13.5%. a) PCA diatom species

(abbreviation are listed in Table 2). b) PCA samples. The influence of environmental variables to the variance of single species within the assemblages is given by the length of the species vectors. Species that plot close to the center of the diagram (i.e. having short lines) are most likely not significantly affected by the environmental gradients. Diatom species that have a small angle between each other in the analysis occur in the same set of samples and thus have similar distribution patterns, whereas species having a large angle between each other tend towards different distribution patterns (a). Similarly, samples that plot close together will contain the same species, whereas samples plotted far apart will contain different species (b). Colored lines group species and stations in zones: SAZ (red), PFZ+POOZ (green), TZ (orange) and sSIZ (blue).

Figure 8. Spearman Principal Component Analysis (PCA) biplot showing the relationship between the 12 measured variables at 51 sampling stations. PC1 represents 44.2% of the variance and PC2 14.1%. Colored symbols group stations in zones: SAZ (red), PFZ+POOZ (green), TZ (orange) and sSIZ (blue). TOC= total organic carbon, TN= total nitrogen, Diat= Diatoms, Pig= Pigments, St= Sterols. Open circles= stations  $\leq 2,500$  m water depth, and closed circles= stations  $> 2,500$  m water depth.

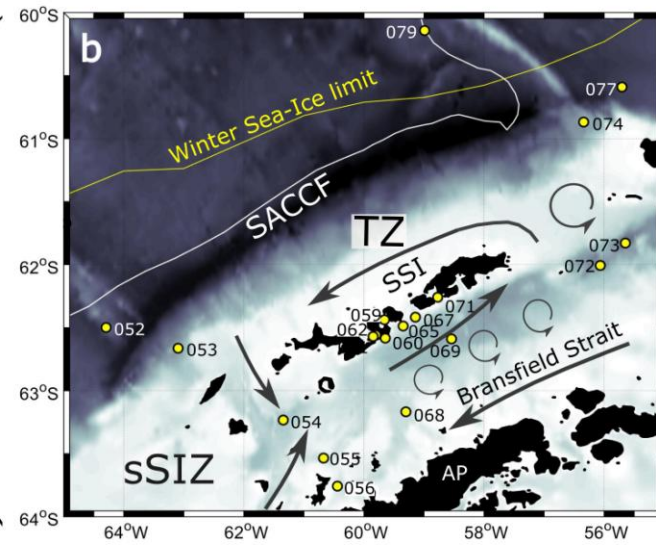
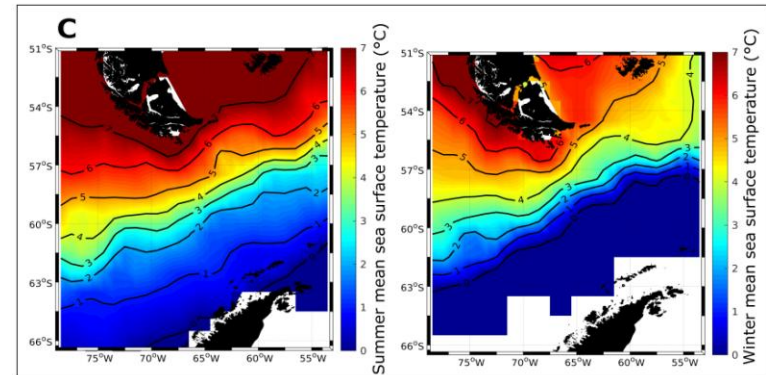
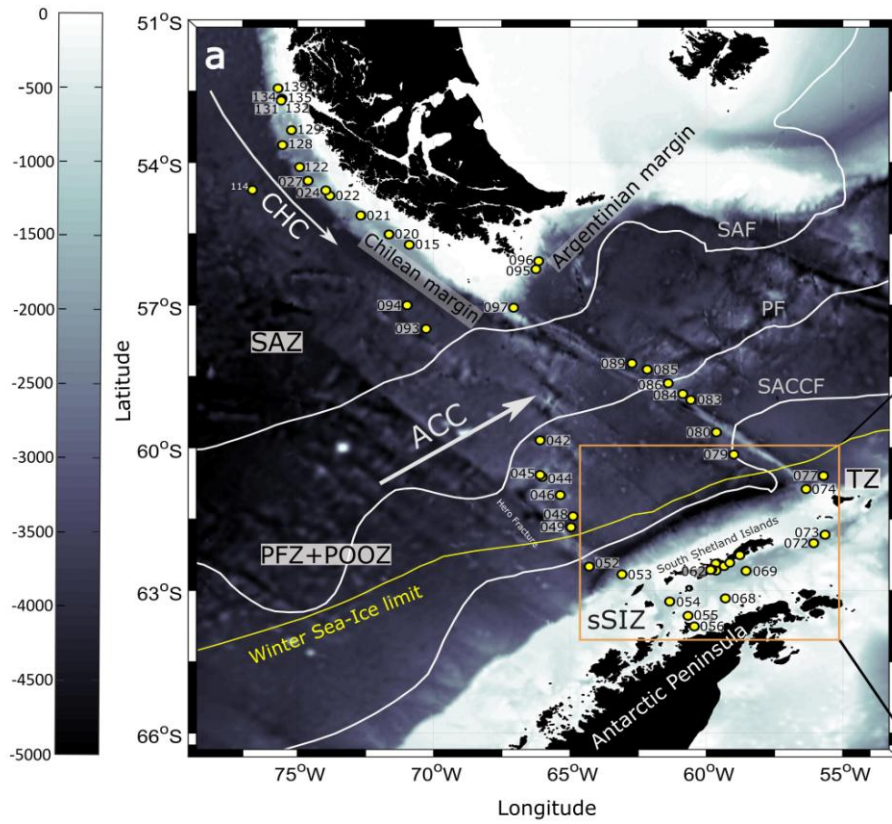
Table 1

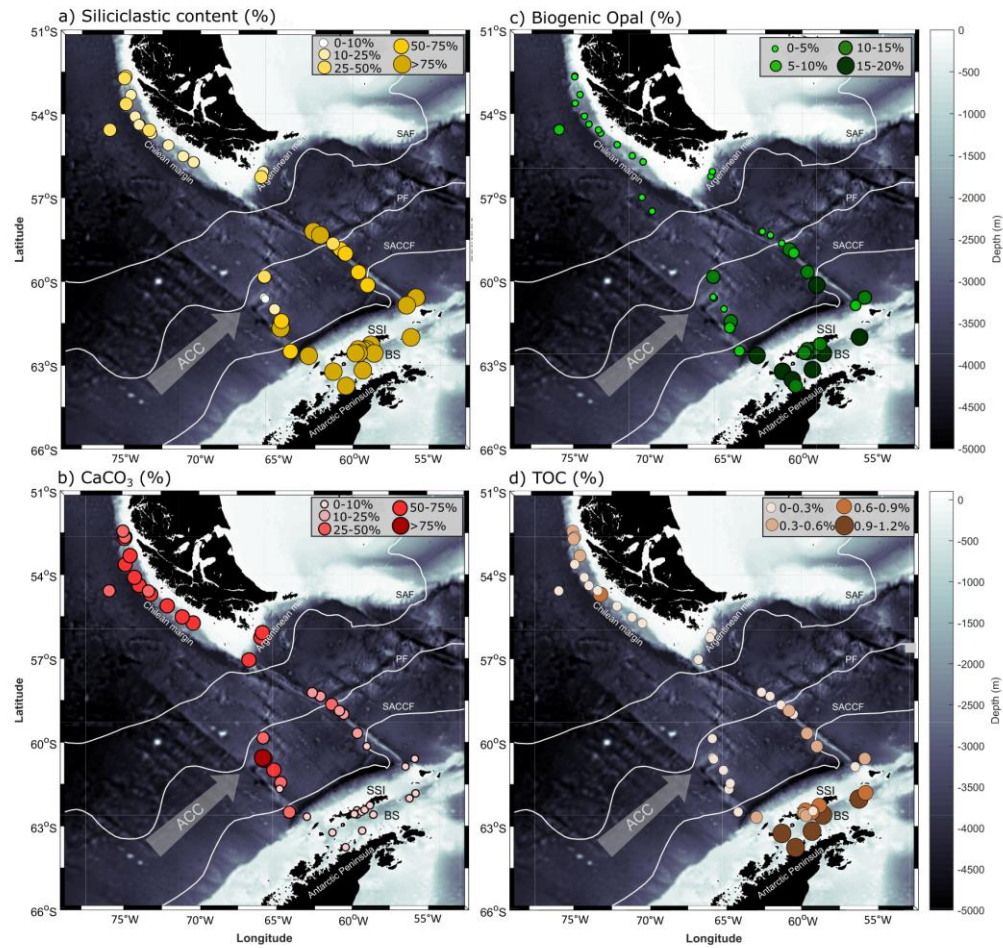
Carbon number	Retention time (min)	Systematic name	Short name	Common name	Source
C <sub>26</sub>	25.65	22,24-cyclocholest-5-ene	Propyl C <sub>26</sub> Δ <sup>5</sup>		Common in organisms higher in the food web. Result from degradation of the side-chain of the dietary microalgal sterols (Volkman, 2003).
	25.75	24-nor-5α-cholest-22-en-3β-ol	C <sub>26</sub> Δ <sup>22</sup>		
C <sub>27</sub>	26.02	cholest-5-en-3β-ol	C <sub>27</sub> Δ <sup>5</sup>	Cholesterol	Biomarker for the eukaryotic marine community (Volkman, 1986) produced by some algae (Volkman, 2003).
	26.11	5α-cholestan-3β-ol	C <sub>27</sub> Δ <sup>0</sup>	Cholestanol	Indicator of oxidation reaction of cholesterol (Gagosian et al., 1980).
	26.41	cholesta-5,24-dien-3β-ol	C <sub>27</sub> Δ <sup>5,24</sup>	Desmosterol	Radial-centric diatoms related to sea-ice (Rampen et al., 2010).
	26.95	cholest-4-en-3-one	C <sub>27</sub> Δ <sup>4</sup>	Cholestenone	Indicator of oxidation reaction of cholesterol (Gagosian et al., 1980).
C <sub>28</sub>	26.45	24-methylcholest-5,22E-dien-3β-ol	C <sub>28</sub> Δ <sup>5,22</sup>	Brassicasterol	Associated with diatoms and <i>Phaeocystis</i> (e.g., Villinski et al., 2008).
	27.04	24-methylcholesta-5,24(28)-dien-3β-ol	C <sub>28</sub> Δ <sup>5,24(28)</sup>	Methylenecholesterol	Derived mainly from planktonic sources and diatom marker (Volkman, 1986, 2003).
	27.13	24-methylcholest-5-en-3β-ol	C <sub>28</sub> Δ <sup>5</sup>	Campesterol	Associated with vascular plants (Volkman, 1986) and diatoms (Villinski et al., 2008).
C <sub>29</sub>	27.48	24 ethylcholest-5,22E-3β-ol	C <sub>29</sub> Δ <sup>5,22</sup>	Stigmasterol	Considered the principal sterol in vascular plants (Volkman, 2003). Also observed in a few diatoms, dinoflagellates and prymnesiophyte algae (Volkman, 1986).
	28.18	24-ethylcholest-5-en-3β-ol	C <sub>29</sub> Δ <sup>5</sup>	β-sitosterol	Associated with vascular plants (Volkman 1986). Also observed in Chlorophyta, cyanobacteria, prymnesiophyte algae, and some diatoms (Volkman, 1986; Villinski et al., 2008).
	29.26	stigmasta-5,24(28)-dien-3β-ol	C <sub>29</sub> Δ <sup>5,24</sup>	Fucosterol	Is the major sterol of nearly all macroscopic brown algae (Phaeophyceae) (Volkman, 1986).
C <sub>30</sub>	28.71	4α,22,23-trimethylcholest-22E-en-3β-ol	C <sub>30</sub> Δ <sup>22</sup>	Dinosterol	Associated mainly with dinoflagellates (e.g., Volkman, 2003) but also reported for raphid diatoms (Rampen et al., 2010).

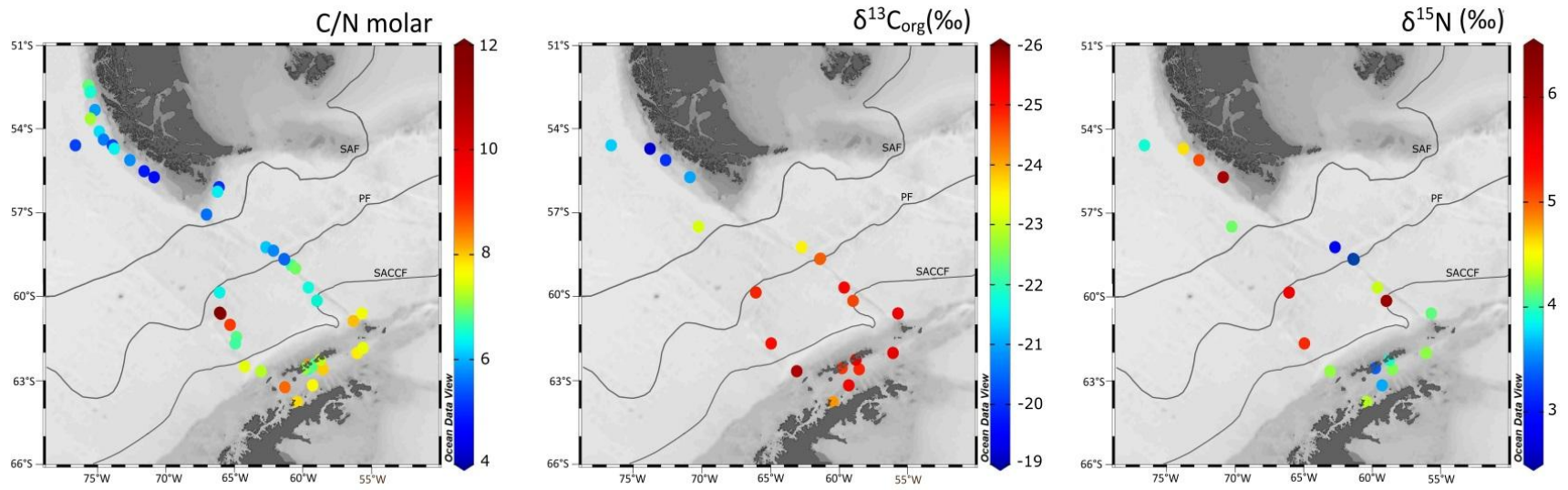
Table 2

Diatom Species Name	Code	Min (%)	Max (%)
<i>Actinocyclus actinochilus</i>	Aacti	0	3.62
<i>Actinocyclus curvatulus</i>	Acurv	0	0.71
<i>Alveus marinus</i>	Amari	0	0.36
<i>Asteromphalus hookeri</i>	Ahook	0	0.20
<i>Asteromphalus parvulus</i>	Aparv	0	0.77
<i>Azpeitia tabularis</i>	Atabu	0	8.48
<i>Chaetoceros</i> spp. (spores)	CRS	0.26	88.92
<i>Chaetoceros</i> spp. (vegetative)	CVS	0	0.98
<i>Corethron pennatum</i>	Cpenn	0	2.95
<i>Coscinodiscus</i> spp.	Cosci	0	0.89
<i>Cyclotella litoralis</i>	Clito	0	0.49
<i>Eucampia antarctica</i> (spore)	Eanta	0	12.62
<i>Fragilariopsis curta</i>	Fcurt	0	8.09
<i>F. cylindrus</i>	Fcyli	0	2.37
<i>F. doliolus</i>	Fdoli	0	0.16
<i>F. kerguelensis</i>	Fkerg	0.25	77.00
<i>F. obliquecostata</i>	Fobli	0	0.77
<i>F. rhombica</i>	Frhom	0	3.14
<i>F. ritscheri</i>	Frits	0	0.44
<i>F. separanda</i>	Fsepa	0	7.58
<i>F. sublinearis</i>	Fsubl	0	0.85
<i>F. vanheurckii</i>	Fvanh	0	1.06
<i>Fragilariopsis</i> spp.	Fspp	0	5.30
<i>Hemidiscus cuneiformis</i>	Hcune	0	0.24
<i>Navicula directa</i>	Ndire	0	0.39
<i>Navicula</i> spp.	Nspp	0	1.77
<i>Nitzschia bicapitata</i>	Nbica	0	0.45
<i>Nitzschia lecointei</i>	Nleco	0	0.13
<i>Nitzschia sicula</i> var. <i>bicuneata</i>	Nsicu	0	0.22
<i>Odontella weissflogii</i>	Oweis	0	5.74
<i>Porosira pseudodenticulata</i>	Ppseu	0	2.16
<i>Proboscia alata</i> sensu Jordan	Palat	0	1.56
<i>Pseudo-nitzschia lineola-turgidula</i> group	Plitu	0	0.39
<i>Pseudo-nitzschia heimii</i>	Pheim	0	0.24
<i>Rhizosolenia antennata</i>	Rante	0	0.20
<i>Rhizosolenia antennata</i> f. <i>semispina</i>	Ranse	0	0.81
<i>Rhizosolenia</i> species A	RspA	0	1.34
<i>Rhizosolenia</i> spp.	Rsppp	0	0.44
<i>Roperia tessellata</i>	Rtess	0	5.34
<i>Stellarima microtrias</i>	Smicro	0	0.76
<i>Stephanopyxis</i> sp.	Stephan	0	1.94
<i>Thalassionema nitzschioides</i> group	Tnigr	0	2.43
<i>T. nitzschioides</i> forma 1	Tnif1	0	3.40
<i>Thalassiosira antarctica</i>	Tanta	0	3.62
<i>T. gracilis</i> group ( <i>Shionodiscus gracilis</i> group)	Tgrac	0	5.12
<i>T. lentiginosa</i>	Tlent	0.36	19.64
<i>T. lineata</i>	Tline	0	0.44
<i>T. oestrupii</i> ( <i>Shionodiscus oestrupii</i> )	Toest	0	1.07
<i>T. oliverana</i>	Toliv	0	0.89
<i>T. trifulta</i> ( <i>Shionodiscus trifultus</i> )	Ttrif	0	1.76
<i>Thalassiosira</i> sp. 3	Tsp3	0	3.34
<i>Thalassiosira</i> spp.	Tspp	0.20	6.94
<i>Thalassiothrix antarctica</i>	Txant	0	0.89

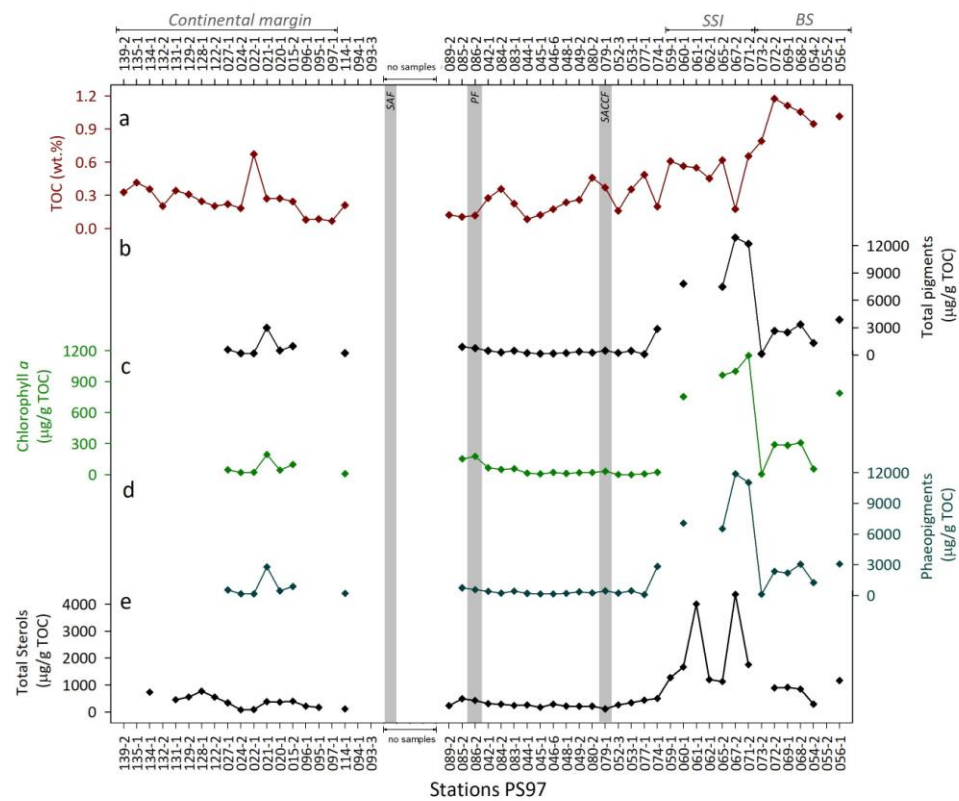


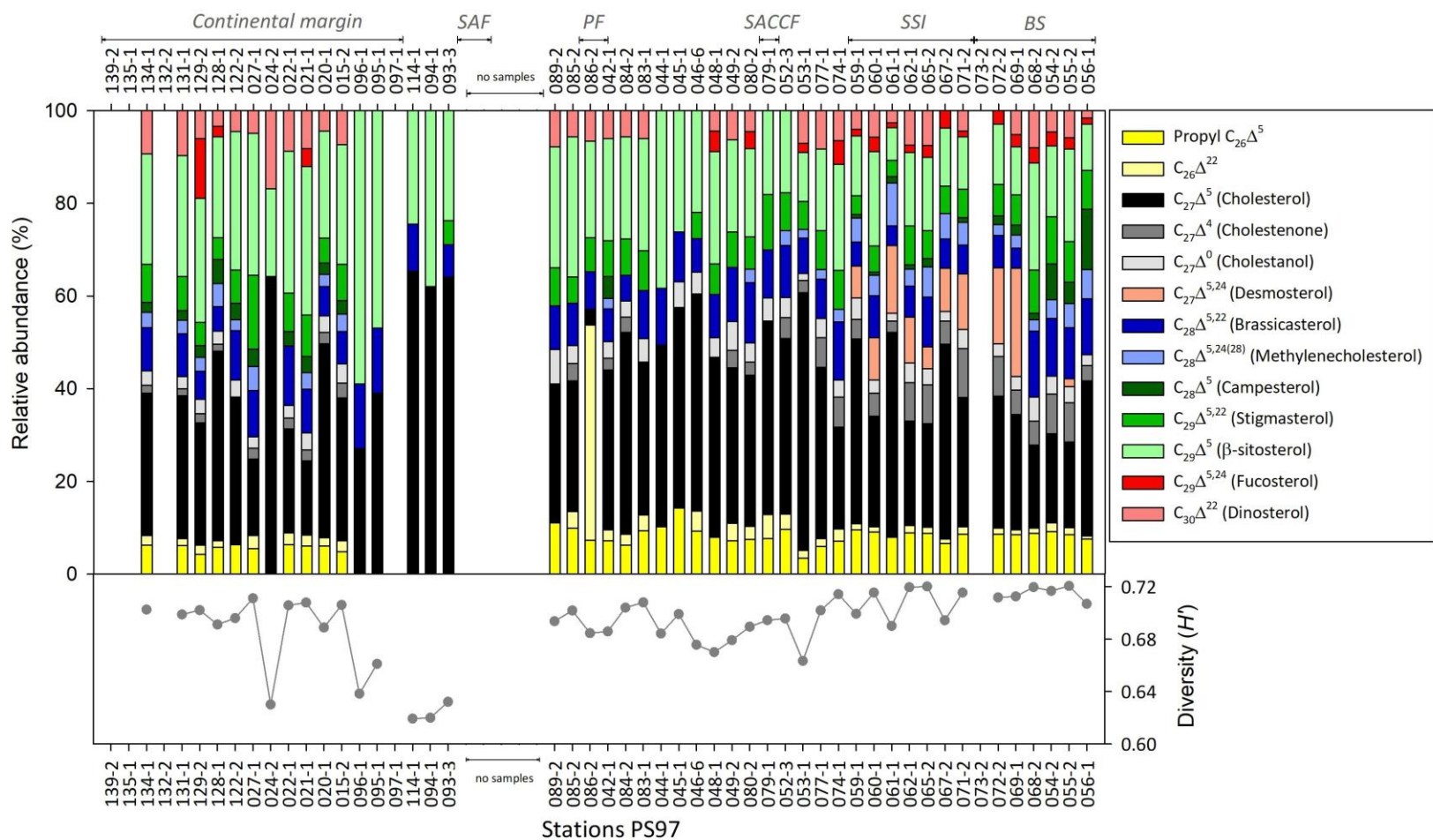


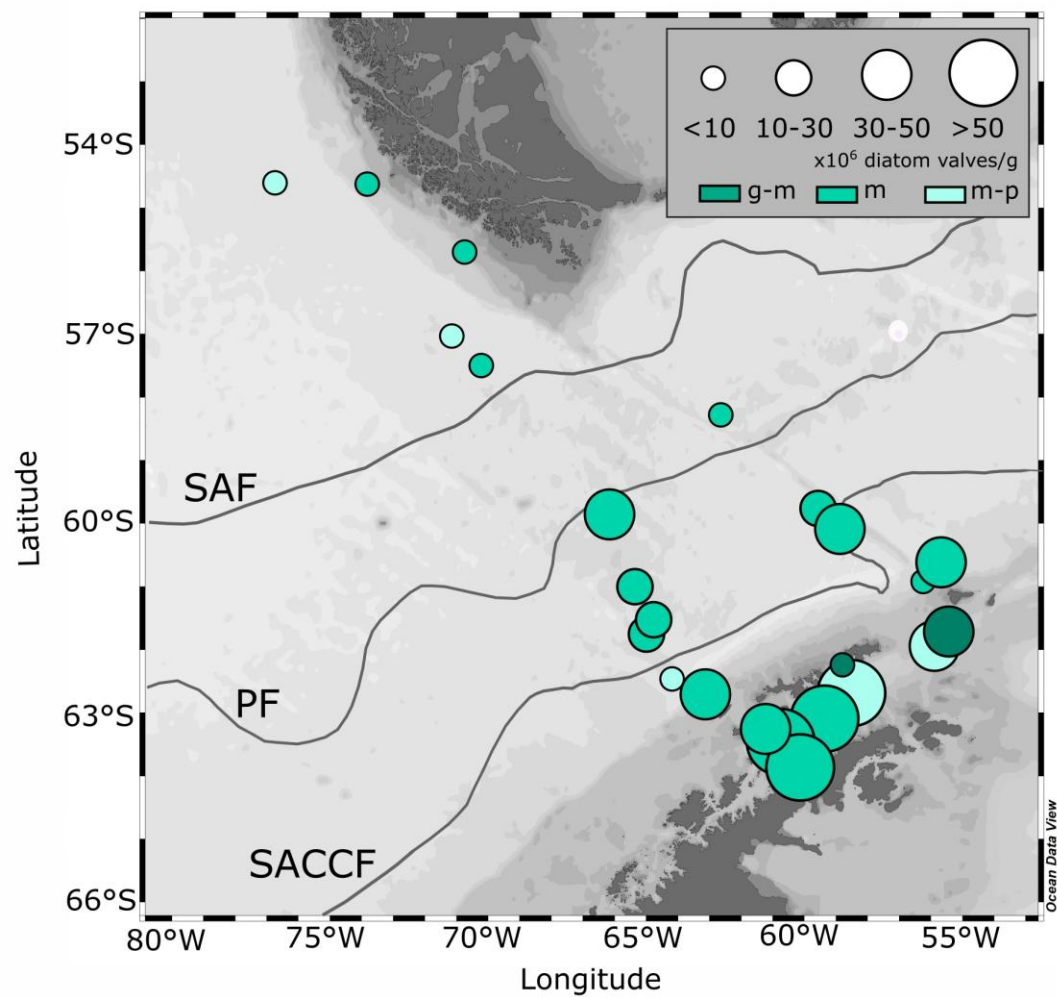


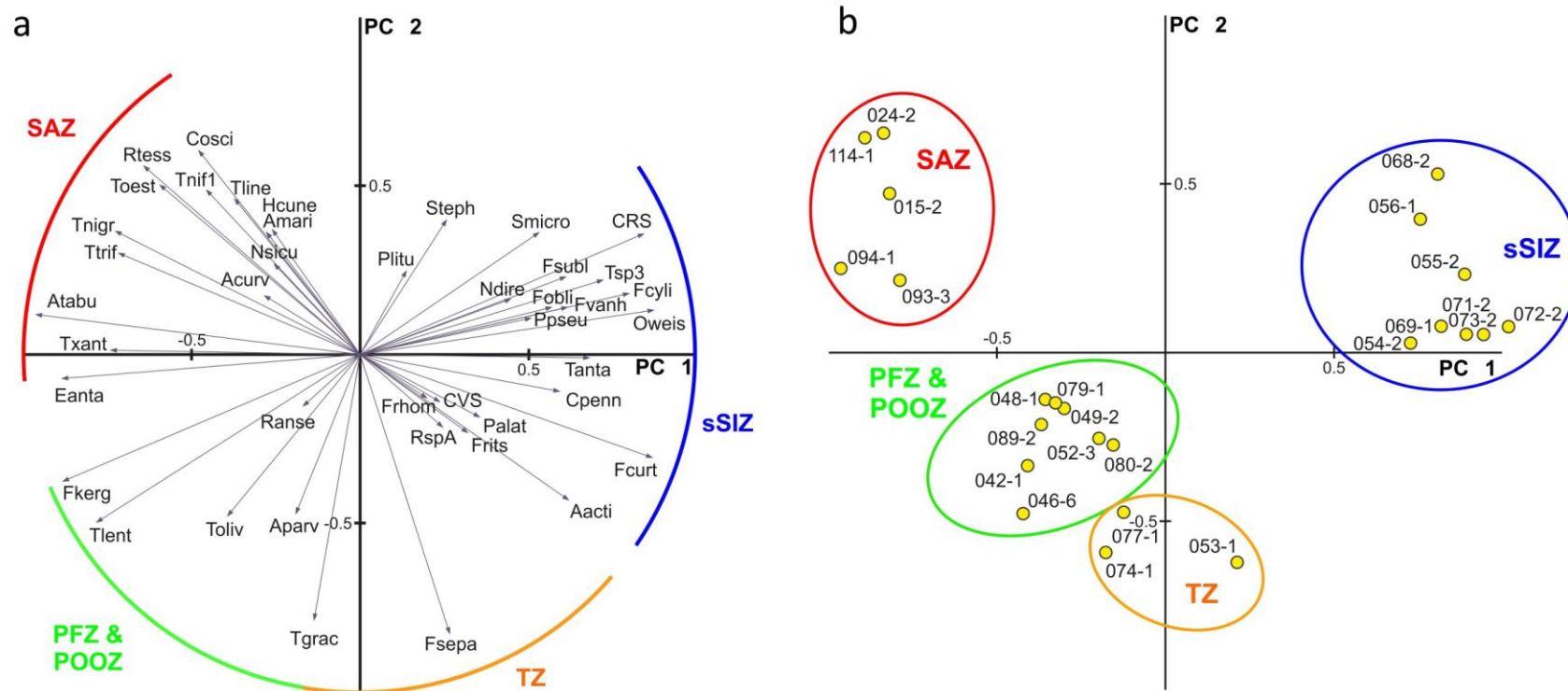


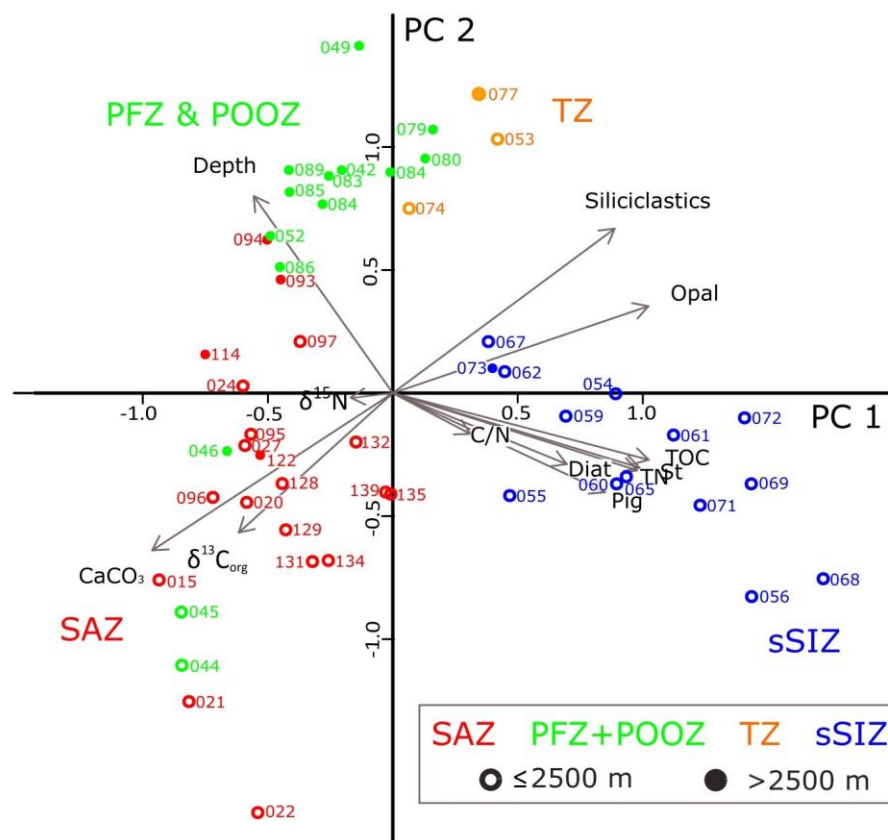
ACCEPTED MANUSCRIPT











**Highlights**

- Latitudinal gradient in sediment composition associated with oceanic fronts
- Diatom concentrations correlated with biogenic opal
- Diatom species distribution reflects N-S environmental gradients
- Pigments and sterols in Bransfield Strait associated with high productivity pulses
- Low chl *a*:phae suggests phytoplankton carbon degradation
- Sterols assigned to different biological sources